P. Collet, M. Courbage, S. Métens, A. Neishtadt, and S. Zaslavsky, Eds.,
Chaotic Dynamics and Transport in Classical and Quantum Systems,
(Kluwer Academic Publishers, Dordrecht, 2005) pp. 107-157.

DYNAMICAL SYSTEMS THEORY OF IRREVERSIBILITY

Pierre Gaspard
Center for Nonlinear Phenomena and Complex Systems,
Faculté des Sciences, Université Libre de Bruxelles,
Campus Plaine, Code Postal 231, B-1050 Brussels, Belgium

Recent work on the connections between dynamical systems theory and nonequilibrium statistical mechanics is reviewed with emphasis on results which are compatible with Liouville's theorem. Starting from a general discussion of time-reversal symmetry in the Newtonian scheme, it is shown that the Liouvillian eigenstates associated with the Pollicott-Ruelle resonances spontaneously break the time-reversal symmetry. We explain that such a feature is compatible with the time reversibility of Newton's equations because of a selection of trajectories which are not time-reversal symmetric. The Pollicott-Ruelle resonances and their associated eigenstates can be constructed not only for decay processes but also for transport processes such as diffusion or viscosity, as well as for reaction-diffusion processes. The Pollicott-Ruelle resonances thus describe the relaxation toward the thermodynamic equilibrium. The entropy production of these relaxation processes can be calculated and shown to take the value expected from nonequilibrium thermodynamics. In nonequilibrium steady states, an identity is obtained which shows that the entropy production directly characterizes the breaking of time-reversal symmetry by nonequilibrium boundary conditions. The extension to quantum systems is also discussed.

I. INTRODUCTION

The methods of dynamical systems theory are ubiquitous in nonequilibrium statistical mechanics since the pioneering work by Sinai and coworkers on the ergodic theory of hard-ball systems [1–4]. The defocusing character of elastic collisions shows that typical many-particle systems have a spectrum of positive Lyapunov exponents and a positive Kolmogorov-Sinai entropy per unit time [5–8]. This chaotic behavior can be expected from the typical master equations ruling the stochastic processes of nonequilibrium statistical mechanics such as the Boltzmann-Lorentz, the Fokker-Planck, or the Pauli equations, which all develop a positive (and even infinite) Kolmogorov-Sinai entropy per unit time [9, 10]. Moreover, a vanishing Kolmogorov-Sinai entropy would be in contradiction with experimental observation [11].

The connection between dynamical systems theory and nonequilibrium statistical mechanics has been strengthened by the discovery of relationships between the decay or escape rates of a system and the characteristic quantities of its dynamical instability, randomness or fractality [12–15]. These characteristic quantities are large-deviation properties of the temporal dynamics. These new relationships are connecting the large-deviation properties of the temporal evolution of the probabilities or phase-space volumes to the irreversible properties such as the transport coefficients or the entropy production. All these new relationships from the escape-rate formula [12–15] to the fluctuation theorem [16–23] share this very same structure, as will be explained later.

Besides, Pollicott and Ruelle have introduced a concept of resonance for Axiom A systems, showing that hyperbolic systems can present exponential decays which are intrinsic to their dynamics and independent of the circumstances of extraneous observation [24–27]. The concept of Pollicott-Ruelle resonance leads to a spontaneous breaking of the time-reversal symmetry in the statistical description of the time evolution, which provides an explanation of irreversibility in agreement with the microreversibility. This explanation has recently been documented in great detail for deterministic diffusive systems with the verification that the decaying modes associated with the Pollicott-Ruelle resonances have the entropy production expected from the irreversible thermodynamics of diffusive processes [28–32]. One of the basic difficulties has here been to respect Liouville's theorem that phase-space volumes are preserved by the microscopic Hamiltonian dynamics. It should here be emphasized that Liouville's theorem is playing a central role in Boltzmann's considerations. The violation of Liouville's theorem by some hypothetical phase-space contraction leads to the catastrophic situation where the differential entropy – which should naturally be associated with the stationary probability distribution of the system itself according to Boltzmann's statistical interpretation – is equal to minus infinity instead of remaining bounded.

The purpose of the present paper is to show that it is possible to develop a theory of irreversibility for an underlying microscopic dynamics which is time-reversal symmetric and moreover preserves the phase-space volumes in conformity

with Liouville's theorem. This allows us to construct, in particular, nonequilibrium steady states with a well-defined entropy. The general idea of the theory is to consider special solutions of Liouville's equation, which are decaying in time. These solutions turn out to be concentrated on the unstable manifolds which are distinct from the stable manifolds. This leads to a natural breaking of the time-reversal symmetry in the statistical description.

The plan of the paper is the following. Elementary considerations on the time-reversal symmetry and its breaking are developed in Sec. II. The general theory is presented in Sec. III. The theory is applied to simple decay processes in Sec. IV. The escape-rate formalism which gives access to the transport coefficients is presented in Sec. V. The hydrodynamic modes of diffusion are constructed for infinite spatially extended systems in Sec. VI. The entropy production is obtained in Sec. VII. The case of nonequilibrium steady states is treated in Sec. VIII. The possible extension to quantum systems is discussed in Sec. IX. Conclusions are drawn in Sec. X.

II. TIME-REVERSAL SYMMETRY AND ITS BREAKING

The phenomenon of spontaneous symmetry breaking is well known. Typically, the solutions of an equation have a lower symmetry than the equation itself. This is in particular the case for the time-reversal symmetry of Newton's equations. The purpose of the present section is to develop this remark, which sheds some light on the apparent dichotomy between the everyday experience of an irreversible world ruled by time-reversible laws.

If we consider a system of particles of masses m_a interacting with electromagnetic or gravitational forces, it is well known that Newton's equations

$$m_a \, \frac{d^2 \mathbf{r}_a}{dt^2} = \mathbf{F}_a \left(\mathbf{r}_1, \mathbf{r}_2, ..., \mathbf{r}_N \right) \qquad (a = 1, 2, ..., N) \tag{1}$$

ruling the motion of the particles is time-reversal symmetric. Time reversal consists in reversing the velocities $\frac{d\mathbf{r}_a}{dt}$ or momenta $\mathbf{p}_a = m_a \frac{d\mathbf{r}_a}{dt}$ of the particles while keeping invariant their positions $\mathbf{r}_a$:

$$\mathbf{\Theta} \left(\mathbf{r}_1, \mathbf{r}_2, ..., \mathbf{r}_N, \mathbf{p}_1, \mathbf{p}_2, ..., \mathbf{p}_N, t \right) = \left(\mathbf{r}_1, \mathbf{r}_2, ..., \mathbf{r}_N, -\mathbf{p}_1, -\mathbf{p}_2, ..., -\mathbf{p}_N, -t \right) \tag{2}$$

Time reversal is an involution: $\mathbf{\Theta}^2 = 1$. We denote by $\mathbf{\Phi}^t$ the flow of trajectories induced by Newton's equations (1) in the phase space of positions and momenta

$$\mathbf{\Gamma} = \left(\mathbf{r}_1, \mathbf{r}_2, ..., \mathbf{r}_N, \mathbf{p}_1, \mathbf{p}_2, ..., \mathbf{p}_N \right) \in \mathcal{M} \tag{3}$$

The phase space $\mathcal{M}$ is made of all the possible physically distinct states of the system. The flow $\mathbf{\Phi}^t$ exists and is unique according to Cauchy's theorem, which is the property of determinism. The time-reversal symmetry of Newton's equations is expressed by

$$\mathbf{\Theta} \circ \mathbf{\Phi}^t \circ \mathbf{\Theta} = \mathbf{\Phi}^{-t} \tag{4}$$

which means that if the phase-space curve

$$\mathcal{C} = \{ \mathbf{\Gamma}_t = \mathbf{\Phi}^t (\mathbf{\Gamma}_0) : t \in \mathbb{R} \} \tag{5}$$

is a solution of Newton's equations, then the time-reversed curve

$$\mathbf{\Theta}(\mathcal{C}) = \{ \tilde{\mathbf{\Gamma}}_{t'} = \mathbf{\Phi}^{t'} \circ \mathbf{\Theta} (\mathbf{\Gamma}_0) : t' \in \mathbb{R} \} \tag{6}$$

starting from the time-reversed initial conditions $\mathbf{\Theta}(\mathbf{\Gamma}_0)$ is also a solution of Newton's equations.

The further question is to know if the solution $\mathcal{C}$ of Newton's equations is or is not identical to its time-reversal image $\mathbf{\Theta}(\mathcal{C})$. If we have a *time-reversal symmetric solution:*

$$\mathcal{C} = \mathbf{\Theta}(\mathcal{C}) \tag{7}$$

the solution has inherited of the time-reversal symmetry of the equation. However, the solution does not have the time-reversal symmetry of the equation if we have a *time-reversal non-symmetric solution:*

$$\mathcal{C} \neq \mathbf{\Theta}(\mathcal{C}) \tag{8}$$

in which case we can speak of the breaking of the time-reversal symmetry by the solution $\mathcal{C}$.

For the one-dimensional harmonic oscillator of Hamiltonian

$$H = \frac{p^2}{2m} + \frac{1}{2} m\omega^2 r^2 \tag{9}$$

or the particle falling with a uniform acceleration

$$H = \frac{p^2}{2m} + mgr \tag{10}$$

all the trajectories are time-reversal symmetric: $\mathcal{C} = \mathbf{\Theta}(\mathcal{C})$, $\forall\, \mathcal{C}$.

In contrast, this is no longer the case for the free particle in uniform motion

$$H = \frac{p^2}{2m} \tag{11}$$

because the solution $r_t = (p_0/m)t + r_0$ is distinct from the time-reversed solution $r_t = -(p_0/m)t + r_0$ (unless the momentum vanishes: $p_0 = 0$). Indeed, the momentum of these solutions points in different spatial directions so that different successions of events happen along these trajectories.

For the inverted harmonic potential

$$H = \frac{p^2}{2m} - \frac{1}{2} m\lambda^2 r^2 \tag{12}$$

or, more generally, for the potential barriers

$$H = \frac{p^2}{2m} + V_0 \exp\left(-\frac{r^{2\nu}}{2a^{2\nu}}\right) - V_0 \qquad\qquad (\nu = 1, 2, ...) \tag{13}$$

the trajectories $\mathcal{C}_E$ with a negative energy E are identical to their time-reversal image: $\mathcal{C}_E = \mathbf{\Theta}(\mathcal{C}_E)$ for $E < 0$. But those with a positive or vanishing energy are not: $\mathcal{C}_E \neq \mathbf{\Theta}(\mathcal{C}_E)$ for $E \geq 0$. In particular, the trajectories with a vanishing energy are the stable $\mathcal{W}_\mathrm{s}$ and unstable $\mathcal{W}_\mathrm{u}$ manifolds of the equilibrium point $r = p = 0$ and they are distinct. The time-reversal symmetry maps these manifolds onto each other

$$\mathcal{W}_\mathrm{u} = \mathbf{\Theta}(\mathcal{W}_\mathrm{s}) \tag{14}$$

and, here, we have that $\mathcal{W}_\mathrm{u} \neq \mathcal{W}_\mathrm{s}$.

In conclusion, the solutions of Newton's equations typically break the time-reversal symmetry notwithstanding the fact that the equation itself possesses the symmetry. This phenomenon is known as spontaneous symmetry breaking and it manifests itself in different contexts.

We owe to Newton – and his contemporaries who cast his laws of motion into differential equations – the separation between the law and its realizations into specific solutions. This is a major historical step with respect to pre-Newtonian science. Newton's ordinary differential equations leave open the determination of the initial conditions which thus remain arbitrary and out of the law in the Newtonian scheme. The few preceding examples suggest that, in typical systems, many initial conditions lead to solutions which are not time-reversal symmetric, i.e., such that $\mathcal{C} \neq \mathbf{\Theta}(\mathcal{C})$. The separation between time-reversible laws and its irreversible realizations thus appears at the origin of problems with the arrows of time, which were absent in pre-Newtonian science. The preceding discussion shows that an irreversible world – which is given by a specific trajectory of Newton's equations – is not incompatible with a time-reversible equation of motion. The phenomenon of spontaneous symmetry breaking should have familiarized us with such an apparent dichotomy.

Similar considerations apply to Liouville's equation ruling the time evolution of statistical ensembles of trajectories in classical statistical mechanics. Liouville's equation is time-reversal symmetric if the underlying Hamiltonian system is.

Similar considerations also apply to Schrödinger's equation of quantum mechanics, as well as to von Neumann-Landau equation of quantum statistical mechanics.

The breaking of the time-reversal symmetry is the feature of transport processes such as diffusion or viscosity. Diffusion is ruled by the irreversible equation

$$\partial_t\, n = \mathcal{D}\, \nabla^2 n \tag{15}$$

for the density $n(\mathbf{r}, t)$ of tracer particles which can be so dilute that they do not interact with each other while they diffuse in the surrounding fluid. The previous discussion suggests that the diffusion equation (15) describes the time evolution of ensembles of trajectories which are not time-reversal symmetric. The anti-diffusion equation

$$\partial_t\, n = -\mathcal{D}\, \nabla^2 n \tag{16}$$

describes the time evolution of the time-reversed trajectories.

The purpose of the following sections is to show how the previous considerations can be developed into a quantitative theory of irreversibility which is not incompatible with the time-reversal symmetry of Newton's equations.

III. GENERAL THEORY

A probability density is associated with a statistical ensemble $\{\mathbf{\Gamma}^{(i)}\}_{i=1}^{\infty}$ of phase-space points as

$$p(\mathbf{\Gamma}) = \lim_{\mathcal{N}\to\infty} \frac{1}{\mathcal{N}} \sum_{i=1}^{\mathcal{N}} \delta\left(\mathbf{\Gamma} - \mathbf{\Gamma}^{(i)}\right) \tag{17}$$

If these points are the initial conditions of trajectories, the probability density evolves in time according to

$$p_t(\mathbf{\Gamma}) = \lim_{\mathcal{N}\to\infty} \frac{1}{\mathcal{N}} \sum_{i=1}^{\mathcal{N}} \delta\left(\mathbf{\Gamma} - \mathbf{\Phi}^t\mathbf{\Gamma}_0^{(i)}\right) \tag{18}$$

The time evolution of this probability density is ruled by Liouville's equation

$$\partial_t\, p = \{H, p\} \equiv \hat{L}p \tag{19}$$

given in terms of the Poisson bracket with the Hamiltonian of the system according to Liouville's theorem, which defines the Liouvillian operator $\hat{L}$. The time integral of Liouville's equation is the Frobenius-Perron operator

$$p_t(\mathbf{\Gamma}) = \hat{P}^t p_0(\mathbf{\Gamma}) = \exp(\hat{L}t)\; p_0(\mathbf{\Gamma}) = p_0(\mathbf{\Phi}^{-t}\mathbf{\Gamma}) \tag{20}$$

The probability density allows us to calculate the mean values of the observables which are functions of the phase-space variables:

$$\langle A\rangle_t = \int A(\mathbf{\Gamma})\; p_t(\mathbf{\Gamma})\; d\mathbf{\Gamma} \tag{21}$$

as well as the time correlation functions $\langle A(0)B(t)\rangle$ or $\langle A(0)A(t)\rangle$.

If the evolution operator is defined on a Hilbert space of phase-space functions, we can define a unitary group of time evolution

$$p_t = \hat{U}^t p_0 = \exp(-i\hat{G}t)\; p_0 \tag{22}$$

with the Hermitian generator given in terms of the Liouvillian operator by

$$\hat{G} = i\hat{L} \tag{23}$$

The resolvent of the Hermitian operator is defined by

$$\hat{R}(z) = \frac{1}{z - \hat{G}} = -i\int_0^{\infty} \mathrm{e}^{izt}\; \mathrm{e}^{-i\hat{G}t}\; dt \tag{24}$$

The unitary operator can be recovered by integration in the complex variable z along the contour $C_+ + C_-$ as

$$\hat{U}^t = \frac{1}{2\pi i}\int_{C_+ + C_-} \mathrm{e}^{-izt}\; \hat{R}(z)\; dz \tag{25}$$

(see Fig. 1). The retarded or advanced evolution operator can be obtained by integrating along the contour $C_\pm$ as

$$\theta(\pm t)\hat{U}^t = \frac{1}{2\pi i}\int_{C_\pm} \mathrm{e}^{-izt}\; \hat{R}(z)\; dz \tag{26}$$

By deforming the contour of integration C_+ to the lower half-plane of the complex variable z, we can pick up the contributions from several complex singularities of the analytic continuation of the resolvent. These complex singularities can be poles, branch cuts, or else. The poles are called the Pollicott-Ruelle resonances [24–27]. The sum

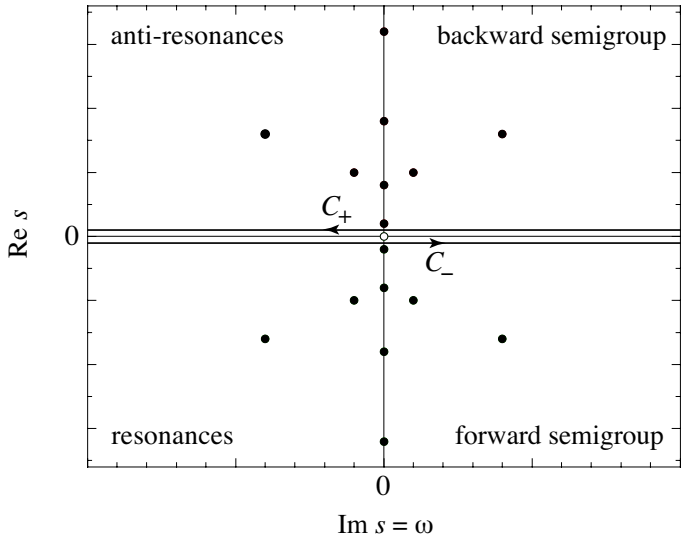

FIG. 1: Complex plane of the variable $s = -iz$. The vertical axis $\mathrm{Re}\, s = \mathrm{Im}\, z$ is the axis of the rates or complex frequencies. The horizontal axis $\mathrm{Im}\, s = -\mathrm{Re}\, z$ is the axis of real frequencies ω. The contour C_+ is slightly above the real-frequency axis and is deformed in the lower half-plane to get the contributions of the resonances for the forward semigroup. The contour C_- is slightly below the real-frequency axis and is deformed in the upper half-plane to get the contributions of the anti-resonances for the backward semigroup. The resonances is mapped onto the anti-resonances by time reversal. Complex singularities such as branch cuts are also possible but not depicted here.

of the contributions from the resonances, the branch cuts, etc... gives us an expansion which is valid for positive times $t > 0$ and which defines the forward semigroup:

$$\langle A\rangle_t = \langle A|\exp(\hat{L}t)|p_0\rangle \simeq \sum_\alpha \langle A|\Psi_\alpha\rangle\ \exp(s_\alpha t)\ \langle\tilde{\Psi}_\alpha|p_0\rangle + \cdots \tag{27}$$

where the dots denote the contributions beside the simple exponentials due to the resonances (see Fig. 1). In such an expansion, the dependence on the observables appears via the right-eigenvectors of the Liouvillian operator

$$\hat{L}|\Psi_\alpha\rangle = s_\alpha|\Psi_\alpha\rangle \tag{28}$$

and the dependence on the initial probability density via the left-eigenvectors

$$\langle\tilde{\Psi}_\alpha|\hat{L} = s_\alpha\langle\tilde{\Psi}_\alpha| \tag{29}$$

On the other hand, the analytic continuation to the upper half-plane of the complex variable z gives an expansion valid for negative times $t < 0$, which defines the backward semigroup:

$$\langle A\rangle_t = \langle A|\exp(\hat{L}t)|p_0\rangle \simeq \sum_\alpha \langle A|\Psi_\alpha\circ\mathbf{\Theta}\rangle\ \exp(-s_\alpha t)\ \langle\tilde{\Psi}_\alpha\circ\mathbf{\Theta}|p_0\rangle + \cdots \tag{30}$$

The time-reversal symmetry implies that a singularity located in the upper half-plane at $-z_\alpha = -is_\alpha$ corresponds to each complex singularity in the lower half-plane of the variable $z_\alpha = is_\alpha$.

The analytic continuation has the effect of breaking the time-reversal symmetry and shows that the semigroups are necessarily restricted to one of the two semi-axes of time.

Several important mathematical questions should be answered in order to obtain such expansions:

- What is the spectrum of complex singularities of the resolvent?
- What is the nature of the right- and left-eigenvectors, Ψ_α and $\tilde{\Psi}_\alpha$, in each term of the expansion? For which class of observables A is defined the right-eigenvector Ψ_α? For which class of initial probability density p_0 is defined the left-eigenvector $\tilde{\Psi}_\alpha$?
- Once each term is well defined, does the whole series converge for some classes of observables A and initial probability densities p_0?

Important results have been obtained for Axiom A systems which is a class of dynamical systems having the properties that:
(1) Their non-wandering set Ω is hyperbolic;
(2) Their periodic orbits are dense in Ω.
For these systems, Pollicott and Ruelle have proved that the spectrum close to the real axis contains resonances (poles) which are independent of the observable and initial probability density within whole classes of smooth enough functions [24–27]. The resonances are responsible for exponential decays $\exp(s_\alpha t)$ at rates $-s_\alpha$ which are thus intrinsic to the dynamics. If the resonances are degenerate of multiplicity m_α, Jordan-block structures may appear which introduce polynomial corrections to the exponential decays, leading to $t^{m_\alpha - 1}\exp(s_\alpha t)$ [10].

In specific systems such as the multibaker maps and the simple examples given in the next section, the whole resonance spectrum as well as the complete expansions of the semigroups have been constructed for very smooth observables and probability density [10, 33, 34]. If the observable and the probability density have a certain degree of regularity, the expansion can be limited to the contributions of the first few resonances plus a rest which decays faster than the decay rate of the last used resonance. This rest becomes negligible after a long enough time.

For non-hyperbolic systems such as intermittent maps or bifurcating equilibrium points, branch cuts appear which are associated with power-law decays [35–38].

An important remark is that the eigenvectors (28) and (29) are not given by functions but by mathematical distributions of the Schwartz type. Therefore, their density does not exist as a function and their cumulative function is required for their representation.

In bounded systems which are mixing, there exists a unique eigenvalue at $s_0 = 0$. The non-trivial Pollicott-Ruelle resonances of the forward semigroup are then located away from the real-frequency axis with $\mathrm{Re}\, s_\alpha < 0$.

However, there exist most interesting situations in which the leading Pollicott-Ruelle resonance has a non-vanishing real part $\mathrm{Re}\, s_0 < 0$. This happens for open systems with escape as shown in Secs. IV and V, as well as for spatially periodic systems as shown in Sec. VI.

In open systems with escape, the leading Pollicott-Ruelle resonance defines the escape rate

$$\gamma = -s_0 \tag{31}$$

The associated eigenvector

$$\hat{P}^t \Psi_0 = \mathrm{e}^{s_0 t}\Psi_0 \tag{32}$$

is given by the conditionally invariant measure of density

$$\Psi_0 = \lim_{t\to\infty} \mathrm{e}^{-s_0 t}\hat{P}^t \Upsilon \tag{33}$$

where Υ is an arbitrary function. The density Ψ_0 is typically singular so that we define the cumulative function

$$F_0(\xi) = \int_0^\xi \Psi_0(\mathbf{\Gamma}_{\xi'})d\xi' \tag{34}$$

where the integral is carried out over a curve $\{\mathbf{\Gamma}_\xi\}$ in the phase space.

In hyperbolic systems, the escape rate can be expressed in terms of the Lyapunov exponents and the Kolmogorov-Sinai entropy per unit time which is defined with respect to the natural invariant measure having the non-wandering set for support [10, 39, 40]:

$$\gamma = \sum_{\lambda_i > 0} \lambda_i - h_{\mathrm{KS}} \tag{35}$$

If we introduce the partial information dimensions $0 \leq d_i \leq 1$ associated with the Lyapunov exponents according to the fundamental work by Young and others [39, 41, 42], the escape rate can be rewritten as

$$\gamma = \sum_{\lambda_i > 0} (1 - d_i)\lambda_i \tag{36}$$

These remarkable formulas generalize Pesin's identity [43]. The escape implies that some partial dimensions are smaller than unity, which shows that the non-wandering set is fractal in some unstable directions as well as in the corresponding stable directions by time-reversal symmetry. In contrast, the conditionally invariant measure associated with the escape rate γ and defined by the density (33) is absolutely continuous with respect to the Lebesgue measure along the unstable directions but fractal in the stable directions.

IV. DECAY PROCESSES

In this section, we consider simple systems with escape of particles from a phase-space region where the non-wandering set is located. The number of particles remaining in this region is decaying so that the process is transient.

A. Inverted harmonic potential

The first example is the Hamiltonian (12) with an inverted harmonic potential. The equilibrium point at $r = p = 0$ constitutes the non-wandering set of this system. The equilibrium point is hyperbolic so that we here have a simple example of Axiom A systems. Its Lyapunov exponents are given by $(+\lambda, -\lambda)$. The invariant measure is a Dirac delta distribution located at the phase-space point $r = p = 0$. Its Kolmogorov-Sinai entropy is equal to zero so that the system is nonchaotic as expected. According to Eqs. (31) and (35), the leading Pollicott-Ruelle resonance should here be given in terms of the positive Lyapunov exponent:

$$s_0 = -\gamma = -\lambda \tag{37}$$

It is straightforward to verify this result and even obtain the full spectrum of the Pollicott-Ruelle resonances together with their associated eigenvectors, as shown here below.

After the canonical transformation

$$\begin{cases} q = \frac{1}{\sqrt{2m\lambda}}(x - y) \\ p = \sqrt{\frac{m\lambda}{2}}(x + y) \end{cases} \tag{38}$$

the Hamiltonian (12) becomes

$$H = \lambda\, x\, y \tag{39}$$

In the new coordinates, the unstable manifold is the axis of the x-coordinate and the stable manifold is the axis of the y-coordinate. The solutions of Hamilton's equations

$$\begin{cases} \dot{x} = +\frac{\partial H}{\partial y} = +\lambda\, x \\ \dot{y} = -\frac{\partial H}{\partial x} = -\lambda\, y \end{cases} \tag{40}$$

define the flow

$$\mathbf{\Phi}^t(x, y) = \left(\mathrm{e}^{+\lambda t} x, \mathrm{e}^{-\lambda t} y\right) \tag{41}$$

In the long-time limit $t \to +\infty$, $\exp(-\lambda t)$ is a small parameter in terms of which we can carried out a Taylor expansion of the statistical averages according to [10]

$$\begin{aligned}
\langle A \rangle_t &= \int dx\, dy\, A\Big(\underbrace{\mathrm{e}^{+\lambda t} x}_{=x'}, \mathrm{e}^{-\lambda t} y\Big)\, p_0(x, y) && (42)\\
&= \mathrm{e}^{-\lambda t} \int dx'\, dy\, A\left(x', \mathrm{e}^{-\lambda t} y\right)\, p_0\left(\mathrm{e}^{-\lambda t} x', y\right) && (43)\\
&= \mathrm{e}^{-\lambda t} \int dx'\, dy \sum_{m=0}^{\infty} \frac{1}{m!}\, \mathrm{e}^{-\lambda m t}\, y^m\, \partial_y^m A(x', 0) \sum_{l=0}^{\infty} \frac{1}{l!}\, \mathrm{e}^{-\lambda l t}\, x'^l\, \partial_x^l p_0(0, y) && (44)\\
&= \sum_{l,m=0}^{\infty} \mathrm{e}^{-\lambda(l+m+1)t}\, \frac{1}{m!} \int dx'\, x'^l\, \partial_y^m A(x', 0)\, \frac{1}{l!} \int dy\, y^m\, \partial_x^l p_0(0, y) && (45)\\
&= \sum_{l,m=0}^{\infty} \mathrm{e}^{-\lambda(l+m+1)t}\, \langle A | \Psi_{lm} \rangle\, \langle \tilde{\Psi}_{lm} | p_0 \rangle && (46)
\end{aligned}$$

We can therefore identify the right- and left-eigenstates as

$$\begin{aligned}
\Psi_{lm}(x, y) &= \frac{1}{m!}\, x^l\, (-\partial_y)^m\, \delta(y) && (47)\\
\tilde{\Psi}_{lm}(x, y) &= \frac{1}{l!}\, y^m\, (-\partial_x)^l\, \delta(x) && (48)
\end{aligned}$$

The eigenstates are given by the derivatives of the Dirac distribution. The right-eigenstates Ψ_{lm} have the unstable manifold $y=0$ for support, while the left-eigenstates $\tilde{\Psi}_{lm}$ have the stable manifold $x=0$ for support. We can check that these distributions are respectively the eigensolutions of the Liouvillian operator and of its adjoint:

$$\hat{L}\ \Psi_{lm} = -\lambda\ (l+m+1)\ \Psi_{lm} \tag{49}$$

$$\hat{L}\ \tilde{\Psi}_{lm} = -\lambda\ (l+m+1)\ \tilde{\Psi}_{lm} \tag{50}$$

Accordingly, the Pollicott-Ruelle resonances of the inverted harmonic potential are simply given by the integer multiples of the Lyapunov exponent λ:

$$s_{lm} = -\lambda\ (l+m+1) \tag{51}$$

with $l,m=0,1,2,3,...$

The right- and left-eigenstates are given by Schwartz distributions defined on smooth enough test functions A and p_0. In order for $\langle A|\Psi_{lm}\rangle$ to be defined, the observable $A(x,y)$ must be m-times differentiable transversally to the unstable manifold $y=0$ and integrable with x^l along the unstable manifold. On the other hand, $\langle\tilde{\Psi}_{lm}|p_0\rangle$ is defined if the probability density $p_0(x,y)$ is l-times differentiable transversally to the stable manifold $x=0$ and integrable with y^m along the stable manifold. The full series (46) converges if $A(x,y)$ is an entire analytic function of exponential type in y and an infinitely differentiable function of compact support in x, while $p_0(x,y)$ is an entire analytic function of exponential type in x and an infinitely differentiable function of compact support in y.

The exponential decay at the escape rate $\gamma=\lambda$ proceeds continuously for the conditionally invariant measure given by the leading right-eigenstate $\Psi_{00}(x,y)=\delta(y)$:

$$\hat{P}^t\Psi_{00} = \mathrm{e}^{-\gamma t}\Psi_{00} \tag{52}$$

This conditionally invariant measure corresponds to a statistical ensemble of trajectories which are uniformly distributed on the unstable manifold $y=0$ and nowhere else. This is an example of selection of trajectories (or initial conditions). The irreversible process of decay is the feature of trajectories located on the unstable manifold $y=0$ which is distinct from the time-reversed manifold $x=0$. The trajectories have been selected by the time evolution. Indeed, if we start from an ensemble of initial conditions located in the vicinity of the equilibrium point $x=y=0$, this cloud of points tends to concentrate along the unstable manifold during the time evolution. In the long-time limit, we obtain with Eq. (33) the leading eigenstate $\Psi_{00}(x,y)=\delta(y)$ which has the unstable manifold for support. This support has a zero Lebesgue measure because the decay process is transient. In this way, we end up in the long-time limit with a time-reversal non-symmetric trajectory associated with the irreversible decay process.

B. Generic potential barrier

A generic potential barrier is defined as a barrier with a quadratic maximum. An example of such potential is given by the Hamiltonian (13) with $\nu=1$. This Hamiltonian system has a unique equilibrium point of saddle type at $r=p=0$ and is a further example of Axiom A system. Here, the Lyapunov exponent is given by

$$\lambda = \sqrt{\frac{V_0}{ma^2}} \tag{53}$$

The Kolmogorov-Sinai entropy is here again vanishing, $h_{\mathrm{KS}}=0$, so that this system is nonchaotic.

The motion in the vicinity of the saddle equilibrium point $r=p=0$ is described by the aforementioned inverted harmonic potential (12). At large distances, the particle is no longer accelerated and moves in free motion contrary to the situation in the inverted harmonic potential, but this difference does not affect the spectrum of Pollicott-Ruelle resonances which is the same in both systems. The spectrum of Pollicott-Ruelle resonances of the generic potential barrier is thus given by

$$s_{lm} = -\lambda\ (l+m+1) \tag{54}$$

with $l,m=0,1,2,3,....$

Accordingly, this system presents a dynamical instability without chaos. Indeed, the particle remains at the top of the hill if it has no momentum, so that $r=p=0$ is a stationary solution. However, perturbed trajectories escape to infinity. Figure 2b depicts different trajectories issued from several initial conditions which are very close to the point $r=p=0$. Figure 2c represents the fraction of trajectories which are still in the interval $-a\leq r\leq +a$ at

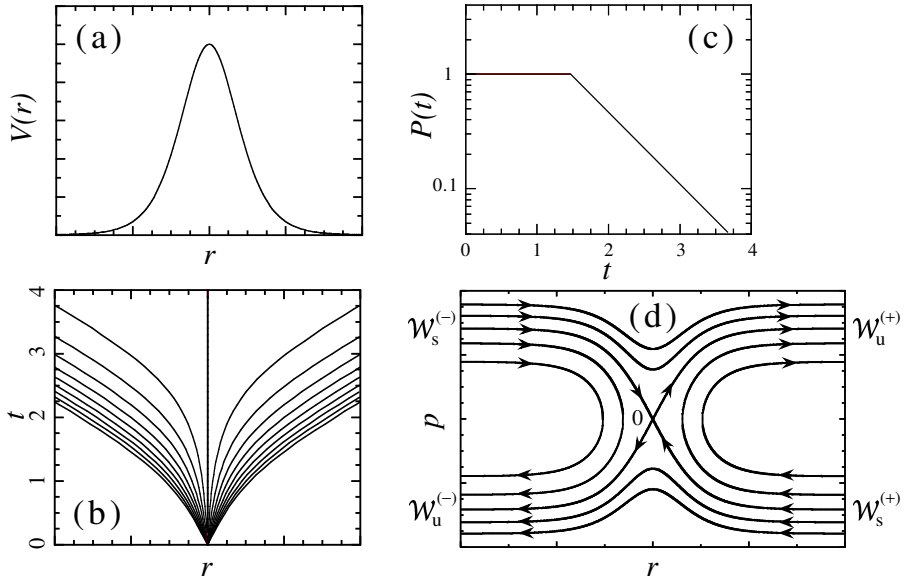

FIG. 2: Particle moving down a hill under the Hamiltonian (13): (a) the potential $V(r)$ versus position r; (b) positions r of different trajectories issued from initial conditions very close to the unstable equilibrium point versus time t; (c) a typical survival probability $P(t)$ versus time t; (d) the phase portrait in the (r,p)-plane with the stable $\mathcal{W}_{\rm s}^{(\pm)}$ and unstable $\mathcal{W}_{\rm u}^{(\pm)}$ manifolds of $r=p=0$.

the current time t. This fraction defines the survival probability. We observe that this survival probability decays exponentially at long times. The rate of decay defines the escape rate γ of the hill. Since the trajectories which escape at very long times are issued from very near the point $r=p=0$, we can understand that the long-time decay is controlled by the dynamical instability near $r=p=0$ and, thus, that the escape rate is equal to the Lyapunov exponent, $\gamma=\lambda$. In Fig. 2d, the phase portrait is drawn in the plane $\mathbf{\Gamma}=(r,p)$. The *stable and unstable manifolds* $\mathcal{W}_{\rm s,u}^{(\pm)}=\{\mathbf{\Gamma}_{\rm s,u}^{(\pm)}(t), t\in\mathbb{R}\}$ are connected to the stationary solution at $\mathbf{\Gamma}=0$. The signs denote both branches of these manifolds.

For $t\to+\infty$, the probability density tends to concentrate along the unstable manifold. We can check that the distribution

$$\Psi_{00}(\mathbf{\Gamma}) \;=\; \sum_{\epsilon=\pm}\int_{-\infty}^{+\infty} \exp(\gamma\tau)\;\delta\left[\mathbf{\Gamma}-\mathbf{\Gamma}_{\rm u}^{(\epsilon)}(\tau)\right]\;d\tau \tag{55}$$

is an exact eigenstate of the Frobenius-Perron operator

$$\hat{P}^t\Psi_{00}(\mathbf{\Gamma}) \;=\; \Psi_{00}(\mathbf{\Phi}^{-t}\mathbf{\Gamma}) \;=\; \exp(-\gamma t)\;\Psi_{00}(\mathbf{\Gamma}) \tag{56}$$

corresponding to the leading Pollicott-Ruelle resonance $s_0=-\gamma=-\lambda$. The result (56) is a consequence of $\mathbf{\Phi}^t\mathbf{\Gamma}_{\rm u}^{(\epsilon)}(\tau)=\mathbf{\Gamma}_{\rm u}^{(\epsilon)}(\tau+t)$ and of the Liouville theorem [44]. The distribution (55) is the density of the conditionally invariant measure associated with the escape rate. We here have a further example of selection of initial conditions. The irreversible character of the escape is the feature of trajectories located on the unstable manifold. The fact that the unstable manifold is distinct from its time reversal – which is the stable manifold – expresses the irreversibility of the escape process and allows for the unidirectional decay (56) in time.

Although the time-reversed process is ideally possible because Hamilton's equations are time-reversal symmetric there are at least two reasons that prevent the realization of such a time-reversed process. A first reason is that dynamical instability can spoil the preparation of a time-reversed state initially prepared in a realistic way. In order to prepare such a state, particles must be placed on their initial conditions. Since the phase space is a continuum, this operation is affected by errors. For the time-reversed state, the initial conditions must be aligned precisely on the stable manifold. But any error transverse to the stable manifold gives to the initial condition a small component in the unstable direction that will be amplified over a time of the order of the inverse of the Lyapunov exponent multiplied by the logarithm of the inverse of the error. Therefore, the cloud of trajectories will be concentrated along the unstable manifold after a time longer than this Lyapunov time and the forward semigroup will anyway control

the long-time evolution. This problem of sensitivity to initial conditions does not manifest itself if the eigenstate is prepared on the unstable manifold because the errors are exponentially damped in this case. The second reason is that the eigenstate (55) belongs to the spectral decomposition of the forward semigroup which is only defined for positive times $t > 0$. On the other hand, the time-reversed eigenstate belongs to the backward semigroup which is defined for negative times $t > 0$. It turns out that the backward semigroup may not be prolongated to positive time because, for typical initial probability densities and observables, the asymptotic series only converges for $t < 0$ and diverges for $t \geq 0$. The origin of time is therefore an unbreakable horizon for the use of the backward semigroup. This horizon is stronger than the horizon due to the positive Lyapunov exponent of a trajectory. Indeed, the Lyapunov horizon can be postponed by taking smaller errors on the initial conditions. In contrast, the horizon of an expansion such as Eq. (46) cannot be postponed.

C. Nongeneric potential barriers

The Hamiltonians (13) with $\nu = 2, 3, 4, ...$ give examples of nonhyperbolic systems which do not satisfy Axiom A. The system is both nonhyperbolic and nonchaotic. The equilibrium point $r = p = 0$ is still unstable but the instability is no longer exponential. The decay is here given by a power law. If we prepare a statistical ensemble of trajectories in the vicinity of the top of the hill and we measure the time $T_{\rm esc}$ taken by these trajectories to escape from the hill, we find that the probability that the escape happens beyond the current time t decays according to the power law

$$\mathrm{Prob}\{T_{\rm esc} > t\} \sim \frac{1}{t^{\frac{1}{\nu-1}}} \tag{57}$$

The decay is no longer exponential so that the resonances of the previous examples are here replaced by a branch cut $\{\mathrm{Re}\, s + i\, \mathrm{Im}\, s : \mathrm{Re}\, s \leq 0, \mathrm{Im}\, s = 0\}$ in the plane of the complex variable s of the Liouvillian resolvent $(s - \hat{L})^{-1}$ for the forward semigroup. By time-reversal symmetry, the spectrum of the backward semigroup has a branch cut in the upper half-plane.

Stable and unstable manifolds are still associated with the equilibrium point $r = p = 0$ and the decay process forward in time will here also be controlled by trajectories concentrated on the unstable manifold and thus distinct from the time-reversed trajectory. Therefore, there is here also a spontaneous symmetry breaking of the time-reversal symmetry but due to an instability which is weaker than exponential. This shows the great generality of the present theory since it may also apply to nonhyperbolic and nonchaotic systems. The difference with respect to hyperbolic systems is that the spectrum of complex singularities controlling the semigroups may be dominated by branch cuts instead of resonances in nonhyperbolic systems. Branch cuts appear in other examples of nonhyperbolic systems such as bifurcating vector fields and intermittent maps [35–38]. Only a precise analysis of the spectrum can determine the long-time behavior of the statistical ensembles of trajectories.

We should notice that, generically, the potential barrier has a quadratic maximum so that exponential decay controlled by Pollicott-Ruelle resonances is the generic behavior in the family of Hamiltonian systems (13). The robustness of hyperbolicity is an important property which has been pointed out in many circumstances.

D. The disk scatterers

The disk scatterers form a family of open dynamical systems with escape which includes chaotic systems. The disk scatterers or disk billiards are Hamiltonian-type systems in which a free particle undergoes elastic collisions on a finite number of immobile hard disks. Energy as well as the phase-space volumes are conserved. Since elastic collisions on circular disks are defocusing these systems are hyperbolic with a positive Lyapunov exponent. Axiom A is satisfied if the disks are sufficiently far apart and do not hide each other. The non-wandering set is composed of the trajectories bouncing forever between the disks. The non-wandering set is of zero Lebesgue measure so that almost all the trajectories escape in free motion to infinity.

A first example is the two-disk scatterer. Here, the non–wandering set is composed of the unique periodic orbit bouncing between the two disks along the line joined their centers. This periodic orbit is unstable with stable and unstable manifold. The situation is similar to the case of the generic potential barrier: the escape rate is equal to the Lyapunov exponent, $\gamma = \lambda$, and the Kolmogorov-Sinai entropy is vanishing, $h_{\rm KS} = 0$. The system is hyperbolic but nonchaotic. The spectrum of Pollicott-Ruelle resonance is however more complicated because of the periodic bouncing motion of frequency ω between both disks:

$$s_{lm} = -\lambda(l + 1) + i\, m\, \omega \tag{58}$$

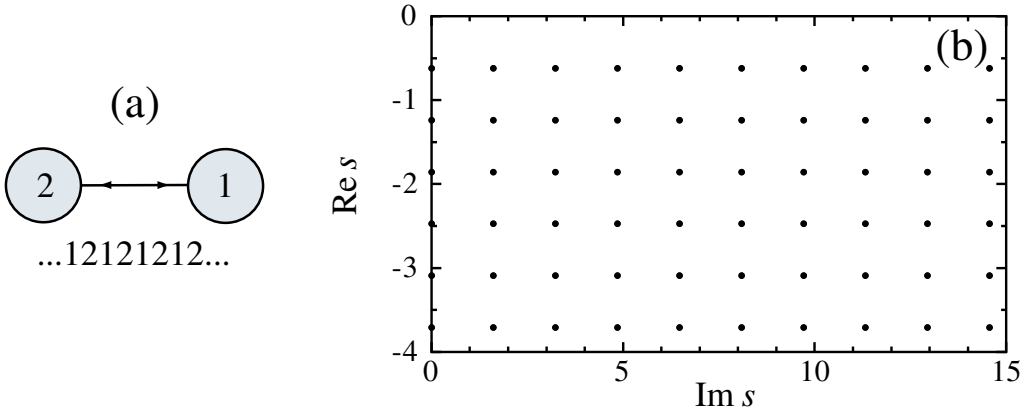

FIG. 3: Two-disk scatterer: (a) configuration of the system; (b) spectrum of Pollicott-Ruelle resonances.

with $l = 0, 1, 2, 3, ...$ and $m = 0, \pm 1, \pm 2, \pm 3, ...$ The resonances form a half periodic array extending toward negative values of Re s and separated from Re $s = 0$ by a gap given by the escape rate $\gamma = \lambda$ (see Fig. 3).

An example of chaotic system is given by the three-disk scatterer. The scatterer is made of three disks at the vertices of an equilateral triangle. After each collision on a disk, the particle has the choice to go to one or the other of the two other disks. This generates an exponential proliferation of possible orbits so that the non-wandering set here contains an uncountable fractal set of trajectories. If the disks are sufficiently far apart, these trajectories can be put in correspondence with a symbolic dynamics. The properties of the three-disk scatterer can be analyzed in great detail [10, 45–47]. The Kolmogorov-Sinai entropy is here positive so that the escape rate is no longer entirely given by the Lyapunov exponent but by the escape-rate formula (35):

$$\gamma = \lambda - h_{\rm KS} \tag{59}$$

The spectrum of Pollicott-Ruelle resonances can be obtained with great precision by periodic-orbit theory (see Fig. 4) [47]. The resonances which are the closest to the real-frequency axis control the decay of statistical ensembles of trajectories escaping the scatterer. Indeed, the survival probability presents an exponential decay modulated by irregular oscillations. The gross exponential decay is controlled by the escape rate while oscillations appear which are the feature of the other Pollicott-Ruelle resonances. This important observation has been obtained in the three- and four-disk scatterers [47].

V. ESCAPE-RATE FORMALISM

The idea of the escape-rate formalism is to consider first-exit problems in deterministic systems sustaining transport processes such as diffusion or viscosity [12–15, 48]. First-exit or first-passage problems are very well known in stochastic theory and reaction-rate theory [49]. First-exit problems have been considered since Kramers' pioneering work [50]. In Kramers' problem, the escape of particles over a barrier is a way to obtain the reaction rate. This problem has many applications in a variety of physical, chemical, and astronomical systems [51]. The aforementioned disk scatterers are simple models of unimolecular reactions [45], but the escape here occurs for a deterministic dynamics. That the transport coefficients can also be obtained by setting up a first-exit problem does not seem to have been largely noticed. The advantage of this method is to work with a finite system on which boundary conditions are imposed. Boundary conditions as well as initial conditions can be changed at will although the equations of motion may not.

A. Viscosity and other transport coefficients

In order to set up a first-exit problem for a given transport property, absorbing boundary conditions should be imposed in the space of variation of the so-called Helfand moment [52], which is the time integral of the corresponding microscopic current [14, 48]. For viscosity, the Helfand moment is given by

$$G = \frac{1}{\sqrt{V k_{\rm B} T}} \sum_{a=1}^{N} x_a p_{ya} \tag{60}$$

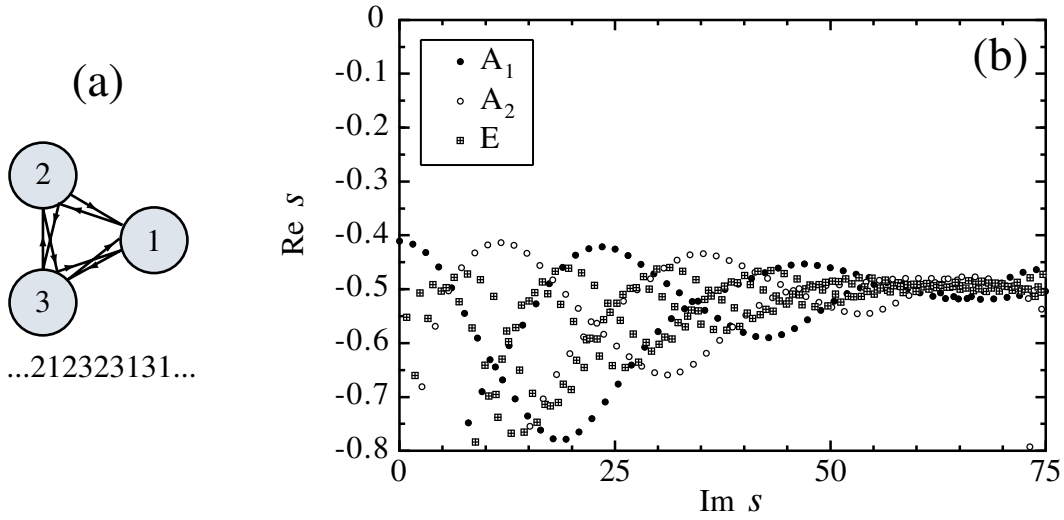

FIG. 4: Three-disk scatterer: (a) configuration of the system; (b) spectrum of Pollicott-Ruelle resonances. A_1, A_2, and E denote the irreducible representations of the group C_{3v} of symmetry of the scatterer with the three disks forming an equilateral triangle. Each resonance belongs to one of these irreducible representations. The A_1- and A_2-resonances are simply degenerate and the E-resonances are doubly degenerate.

where T is the temperature, V the volume of the system, and k_{B} Boltzmann's constant. This Helfand moment gives the center along the x-axis of the y-component of the momenta of the particles. The shear viscosity coefficient is known to be given by the Einstein type of formula

$$\eta = \lim_{t\to\infty} \frac{1}{2t} \langle (G_t - G_0)^2 \rangle \tag{61}$$

There exists a Helfand moment associated with each transport coefficient [52]. Einstein's formula (61) shows that the Helfand moment has a diffusive motion. The corresponding diffusivity coefficient is simply given by the viscosity coefficient according to Eq. (61). We can set up a first-exit problem by considering the escape of trajectories out of the interval $-\frac{\chi}{2} < G < +\frac{\chi}{2}$ in the space of variation of the Helfand moment. The escape rate is directly proportional to the viscosity coefficient and inversely propertional to the square of the distance between the absorbing boundaries at $\pm\frac{\chi}{2}$:

$$\gamma \simeq \eta \left(\frac{\pi}{\chi}\right)^2 \tag{62}$$

We may now consider the same problem for the underlying deterministic dynamics in the phase space of this N-particle system [12–15]. In the phase space $\mathbb{R}^{6N}$, the absorbing boundaries are imposed on the hypersurfaces

$$G = \frac{1}{\sqrt{V k_{\mathrm{B}} T}} \sum_{a=1}^{N} x_a p_{ya} = \pm \frac{\chi}{2} \tag{63}$$

We can consider the set of trajectories forever trapped between these hypersurfaces. We should here point out that, in the three-dimensional physical space, the particles are in a box of finite volume V and they bounce on the walls of the box so that trajectories exist for which the Helfand moment can remain in a compact phase-space region such as the region between the hypersurfaces (63). If the dynamics is hyperbolic, the trajectories which never escape this region are unstable and form a subset of vanishing probability in the phase space. Almost all trajectories escape from this region with an escape rate γ which can be estimated by Eq. (62).

On the other hand, the escape rate is given by dynamical systems theory as the difference between the sum of positive Lyapunov exponents and the Kolmogorov-Sinai entropy according to Eq. (35) or in terms of the partial information dimensions by Eq. (36). Combining with the result (62), we obtain a relationship between the transport coefficient and the characteristic quantities of chaos:

$$\eta = \lim_{\chi\to\infty} \lim_{V,N=nV\to\infty} \left(\frac{\chi}{\pi}\right)^2 \left[\sum_{\lambda_i>0} (1-d_i)\lambda_i\right]_{V,\chi} \tag{64}$$

This formula has recently been used to calculate the viscosity coefficients in a hard-disk model of fluid [48].

An important remark is that irreversible properties such as the transport coefficients already appear in systems with few particles if the dynamics is spatially extended by periodic boundary conditions. This is well known for diffusion in the Lorentz gases but it also true for the other transport coefficients. This is natural because the transport coefficients are routinely computed by molecular dynamics with periodic boundary conditions. It is important to increase the number of particles in the computation in the regimes where the collective effects become essential at high densities n, but the transport properties can already be obtained from the collision between two or three particles at low densities [53].

The escape-rate formalism has the advantage of displaying the irreversibility in the leading Pollicott-Ruelle resonance. In closed systems, the leading Pollicott-Ruelle resonance is vanishing and the interesting behavior is hidden in the next-to-leading resonance. By imposing absorbing boundary conditions, the irreversible behavior is promoted to the leading resonance. For the first-exit problem of viscosity of escape rate (62), the spectrum of Pollicott-Ruelle resonances can be expected to be given by

$$s_j \simeq -\eta \left(\frac{\pi j}{\chi}\right)^2 \tag{65}$$

with $j = 1, 2, 3, ...$, if the system is hyperbolic. The associated right-eigenstates and, in particular, the conditionally invariant measure associated with the leading Pollicott-Ruelle resonance $s_1 = -\gamma$, is smooth in the unstable directions but fractal in the stable ones [13]. This measure decays according to Eq. (32) for $t \to +\infty$. The time-reversed measure belongs to the backward semigroup and is clearly distinct from the conditionally invariant measure of the forward semigroup. We here have another manifestation of the spontaneous breaking of the time-reversal symmetry: this one explicitly for transport properties.

B. Diffusion and mobility

The escape-rate formalism can be applied to a broad variety of situations. For diffusion in a two-degree-of-freedom system such as the Lorentz gas, the Helfand moment is just given by the position of the tracer particle $G_t = x_t$ and Einstein's formula (61) gives the diffusion coefficient $\mathcal{D}$. Alternatively, the diffusion coefficient can be given by Eq. (64) where the partial information dimension can be replaced by the partial Hausdorff dimension $0 \leq d_{\rm H} \leq 1$ in the unique unstable direction of Lyapunov exponent λ [12]

$$\mathcal{D} = \lim_{L\to\infty} \left(\frac{L}{\pi}\right)^2 \left[\lambda(1 - d_{\rm H})\right]_L \tag{66}$$

which has been applied to the hard-disk Lorentz gas [13].

We can also consider the mobility μ in a conservative Lorentz gas with an external electric field $\mathbf{F}$ [10, 54]. On large spatial scales, this process is described by the biased diffusion equation

$$\partial_t\, n = \nabla \cdot (\mathcal{D}\nabla n - \mu \mathbf{F} n) \tag{67}$$

where μ is the mobility coefficient. If two absorbing boundaries are placed at a distance L from each other and transverse to the electric field $\mathbf{F}$, the escape rate is given by

$$\gamma \simeq \mathcal{D}\left(\frac{\pi}{L}\right)^2 + \frac{\mu^2 F^2}{4\mathcal{D}} \tag{68}$$

By combining with the escape-rate formula (35), the diffusion coefficient can be obtained in the limit

$$\mathcal{D} = \lim_{L\to\infty} \lim_{F\to 0} \left(\frac{L}{\pi}\right)^2 \left(\sum_{\lambda_i>0} \lambda_i - h_{\rm KS}\right)_{L,F} \tag{69}$$

and, thereafter, the mobility coefficient in the limit

$$\mu^2 = \lim_{F\to 0} \lim_{L\to\infty} \frac{4\mathcal{D}}{F^2} \left(\sum_{\lambda_i>0} \lambda_i - h_{\rm KS}\right)_{L,F} \tag{70}$$

Other problems can be envisaged with similar considerations.

C. Reaction-diffusion

Reaction-diffusion processes have also been considered in which a point particle undergoes elastic collisions in a hard-disk Lorentz gas with sinks [55, 56]. The sinks are circular holes replacing some disks in the Lorentz gas. If we denote by X a moving point particle and by $\emptyset$ its annihilation, the reaction scheme is given by

$$X + \text{disk} \;\rightleftharpoons\; X + \text{disk} \tag{71}$$

$$X + \text{sink} \;\rightarrow\; \emptyset + \text{sink} \tag{72}$$

Accordingly, the number of point particles in the Lorentz gas decreases with time because of their annihilation at the sinks. This decrease is characterized by the survival probability of a point particle. The time evolution of this survival probability depends on the geometry of the Lorentz gas.

For a Lorentz gas with a periodic lattice of disks and a periodic superlattice of sinks, the same cell containing one sink and several disks repeats itself in a superlattice over the whole system. In this case, the decay is exponential and an escape rate γ can be defined:

$$\text{periodic geometry:} \qquad P(t) \sim \exp(-\gamma t) \tag{73}$$

If the sinks are sufficiently far apart and form a triangular superlattice, the escape rate can be evaluated in terms of the diffusion coefficient $\mathcal{D}$ of the periodic Lorentz gas as

$$\gamma \simeq (14.0 \pm 0.4)\, \frac{\mathcal{D}\, n_\mathrm{s}}{\ln \frac{n_\mathrm{d}}{n_\mathrm{s}}} \tag{74}$$

where n_s is the density of sinks and n_d the density of disks [55]. The trajectories which never escape form a fractal repeller in the three-dimensional phase space of an energy shell. The Hausdorff dimension in this phase space is equal to $D_\mathrm{H} = 2d_\mathrm{H} + 1$ where $0 \leq d_\mathrm{H} \leq 1$ is the partial Hausdorff dimension in the stable or unstable directions. This partial dimension is given in terms of the escape rate (74) and the Lyapunov exponent of the Lorentz gas as

$$d_\mathrm{H} \simeq 1 - \frac{\gamma}{\lambda} \qquad \text{for} \quad n_\mathrm{s} \to 0 \tag{75}$$

For a d-dimensional Lorentz gas with a random configuration of sinks, the survival probability decays according to a stretched exponential [57]

$$\text{random geometry:} \qquad P(t) \sim \exp\left(-C_d\, t^{\frac{d}{d+2}}\right) \tag{76}$$

with a coefficient depending on the concentration of sinks as $C_d \sim |\ln(1 - n_\mathrm{s}/n_\mathrm{d})|^{\frac{2}{d+2}}$. Such a stretched exponential finds its origin in a branch cut in the complex plane s of the Liouvillian spectrum. The density of escape rates $\gamma = -s$ along this branch cut such that

$$P(t) = \int_0^\infty d\gamma\; \rho(\gamma)\; \exp(-\gamma t) \tag{77}$$

presents the Lifchitz tail

$$\rho(\gamma) \sim \exp\left(-\frac{A_d}{\gamma^{\frac{d}{2}}}\right) \tag{78}$$

with a coefficient A_d related to C_d. In $d = 2$, the trajectories which never escape form a set of zero Lebesgue measure but of Hausdorff dimension equal to the phase-space dimension. Indeed, we can here evaluate the number $N(\epsilon)$ of cells of size ϵ required to cover the non-escaping set as [56]

$$N(\epsilon) \sim \frac{1}{\epsilon^3} \exp\left(-2C_2 \sqrt{\frac{1}{\lambda} \ln \frac{1}{\epsilon}}\right) \tag{79}$$

where λ is the Lyapunov exponent. This number increases as $\epsilon \to 0$ more slowly than for a plain three-dimensional object so that the non-escaping set is a fractal but its dimension is nevertheless equal to $D_\mathrm{H} = 3$ [56].

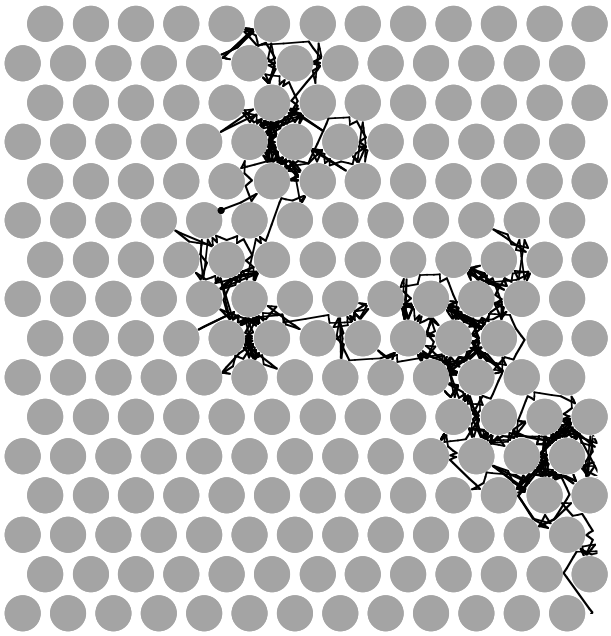

FIG. 5: Periodic hard-disk Lorentz gas: Example of trajectory of a point particle elastically bouncing in a triangular array of immobile hard disks. The distance between the disks does not allow trajectories to cross the lattice without collision so that typical motion is diffusive [3].

VI. HYDRODYNAMIC AND OTHER RELAXATION MODES

A. Lattice Fourier transform

There is another way to promote the irreversibility to the leading Pollicott-Ruelle resonance. If the dynamics is spatially periodic as it is the case for the periodic Lorentz gases (see Fig. 5), we may still consider probability densities which are not necessarily periodic in space. The probability density extends over the infinite system and can be decomposed into Fourier components by a lattice Fourier transform. A remarkable property is that each Fourier component obeys a time evolution which is independent of the other components [10]. The Frobenius-Perron operator ruling the time evolution of a Fourier component depends on its wavenumber $\mathbf{k}$. Accordingly, the Pollicott-Ruelle resonances now depend on the wavenumber. If the wavenumber is vanishing, we recover the dynamics with periodic boundary conditions which admits an invariant probability measure describing the microcanonical equilibrium state. In contrast, an invariant probability measure no longer exists as soon as the wavenumber is non-vanishing. Instead, we find a conditionally invariant complex measure which decays at a rate given by a non-trivial leading Pollicott-Ruelle resonance $s_{\mathbf{k}}$. This conditionally invariant measure defines the hydrodynamic mode of wavenumber $\mathbf{k}$ and the associated Pollicott-Ruelle resonance $s_{\mathbf{k}}$ gives the dispersion relation of the hydrodynamic mode [10].

The hydrodynamic mode of wavenumber $\mathbf{k}$ is an eigenstate of the operator $\hat{T}_{\mathbf{l}}$ of translation by the lattice vector $\mathbf{l} \in \mathcal{L}$:

$$\hat{T}_{\mathbf{l}} \, \Psi_{\mathbf{k}} = \mathrm{e}^{i\mathbf{k}\cdot\mathbf{l}} \, \Psi_{\mathbf{k}} \tag{80}$$

This condition can be called a quasiperiodic boundary condition because it imposes on the state a periodicity of wavelength $2\pi/k$ beside the intrinsic spatial periodicity of the system (which is for instance the size of the lattice cells in the periodic Lorentz gases). The translation operator commutes with the Frobenius-Perron operator

$$\left[\hat{T}_{\mathbf{l}}, \hat{P}^t\right] = 0 \tag{81}$$

so that we may find an eigenstate common to both the spatial translations and the time evolution:

$$\hat{P}^t \, \Psi_{\mathbf{k}} = \mathrm{e}^{s_{\mathbf{k}} t} \, \Psi_{\mathbf{k}} \tag{82}$$

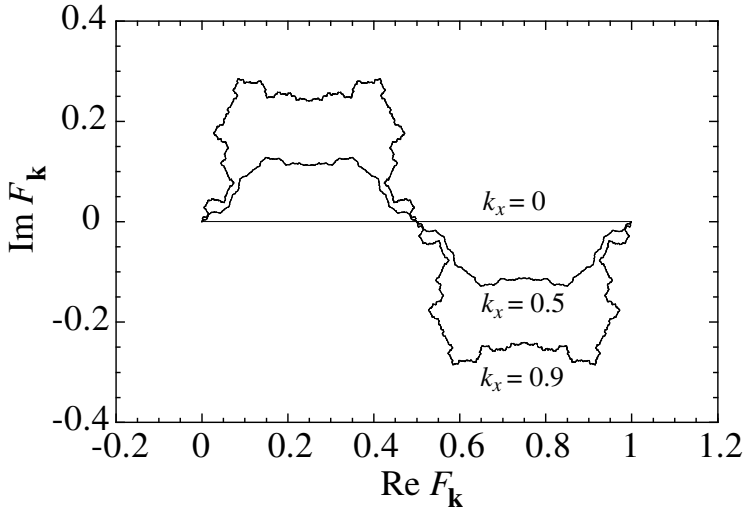

FIG. 6: Periodic hard-disk Lorentz gas: Curves of the cumulative functions of the hydrodynamic modes of wavenumber $k_x = 0.0$, 0.5, and 0.9 with $k_y = 0$ [59].

B. Diffusion

For the periodic Lorentz gases, the leading Pollicott-Ruelle resonance is nothing else than the dispersion relation of diffusion given by van Hove formula [58] as

$$s_{\mathbf{k}} = \lim_{t\to\infty} \frac{1}{t} \ln\langle \exp\left[i\mathbf{k}\cdot(\mathbf{r}_t - \mathbf{r}_0)\right]\rangle = -\mathcal{D}k^2 + O(k^4) \tag{83}$$

where $\mathbf{r}$ is the position of the tracer particle in diffusive motion and $\mathcal{D}$ is the diffusion coefficient. The Pollicott-Ruelle resonance coincides with the eigenvalue $s_0 = 0$ of the microcanonical equilibrium state if the wavenumber vanishes. However, we observe that the Pollicott-Ruelle resonance depends on the wavenumber and becomes non-trivial for non-vanishing wavenumber. This behavior is in contrast to what happens in closed systems where the interesting Pollicott-Ruelle resonances are next-to-leading beside the zero eigenvalue corresponding to the invariant probability distribution. The present considerations with quasiperiodic boundary conditions greatly simplify the use of the Pollicott-Ruelle resonances.

The eigenstate $\Psi_{\mathbf{k}}$ can be considered as a conditionally invariant complex measure, which is smooth in the unstable directions but singular in the stable ones. In general, this eigenstate is a mathematical distribution of Schwartz type which cannot be represented unless integrated in phase space with some test function. For instance, we may consider the cumulative function

$$F_{\mathbf{k}}(\xi) = \int_0^\xi \Psi_{\mathbf{k}}(\mathbf{\Gamma}_{\xi'})\, d\xi' \tag{84}$$

where $\mathbf{\Gamma}_\xi$ is a curve of parameter ξ in the phase space. In the case of diffusion in the periodic Lorentz gases, such cumulative functions can be directly defined as [59]

$$F_{\mathbf{k}}(\theta) = \lim_{t\to\infty} \frac{\int_0^\theta d\theta' \exp\left[i\mathbf{k}\cdot(\mathbf{r}_t - \mathbf{r}_0)_{\theta'}\right]}{\int_0^{2\pi} d\theta' \exp\left[i\mathbf{k}\cdot(\mathbf{r}_t - \mathbf{r}_0)_{\theta'}\right]} \tag{85}$$

with integration on initial positions at an angle $\xi = \theta$ with the horizontal axis and radial initial velocities around a scattering center. The purpose of the denominator is to compensate the exponential decay $\exp(s_{\mathbf{k}}t)$ of the numerator in order to define a function in the limit $t \to \infty$.

For zero wavenumber $\mathbf{k} = 0$, we recover the microcanonical equilibrium state. Indeed, the cumulative function (85) is now given by

$$F_0(\theta) = \frac{\theta}{2\pi} \tag{86}$$

which is the real cumulative function of a uniform probability density $\Psi_0(\theta) = \frac{1}{2\pi}$. If the wavenumber is non-zero, the cumulative function is complex and depicts a fractal curve in the complex plane. The fractal character of the curve tends to increase with the wavenumber as observed in Fig. 6. In order to determine the fractal Hausdorff dimension of this curve, we introduce the Ruelle topological pressure for two-degree-of-freedom systems [60]

$$P(\beta) \equiv \lim_{t\to\infty} \frac{1}{t} \ln \langle |\Lambda_t|^{1-\beta} \rangle \tag{87}$$

where $|\Lambda_t| > 1$ is the stretching factor of a given trajectory, by which an error on the initial condition is amplified after a time t. The Ruelle topological pressure is the generating function of the mean Lyapunov exponent and its statistical moments. The Ruelle topological pressure is equivalently given by

$$P(\beta) = h_{\rm KS}(\beta) - \beta\, \lambda(\beta) \tag{88}$$

in terms of the mean Lyapunov exponent and Kolmogorov-Sinai entropy of an invariant measure μ_β which gives a relative probability weight $|\Lambda_t|^{-\beta}$ to each trajectory [10, 15]. The natural invariant measure of the Liouvillian dynamics is the one with $\beta = 1$. It was proved in Ref. [59] that, for Axiom A systems, the Hausdorff dimension $D_{\rm H}$ of the fractal curve corresponding to the cumulative function of a diffusive hydrodynamic mode of wavenumber $\mathbf{k}$ is given by the root of

$$P(D_{\rm H}) = D_{\rm H}\, {\rm Re}\, s_{\mathbf{k}} \tag{89}$$

where the left-hand side involves the Ruelle topological pressure and the right-hand side the leading Pollicott-Ruelle resonance, i.e., the dispersion relation of diffusion. In the limit of a vanishing wavenumber, the dispersion relation of diffusion vanishes because of Eq. (83) so that the dimension is equal to unity by the property that $P(1) = 0$ in the microcanonical equilibrium state. If we now expand Eq. (89) in powers of $\mathbf{k}^2$, we obtain the Hausdorff dimension as [59, 61]

$$D_{\rm H} = 1 + \frac{\mathcal{D}}{\lambda}\mathbf{k}^2 + O(\mathbf{k}^4) \tag{90}$$

in terms of the diffusion coefficient $\mathcal{D}$ and the mean Lyapunov exponent $\lambda = -P'(1)$. This relationship is in agreement with numerics [59]. This Hausdorff dimension is larger than unity and increases with the wavenumber. It can be rewritten in the form

$$\mathcal{D} = \lim_{\mathbf{k}\to 0} \frac{1}{\mathbf{k}^2}\, \lambda (D_{\rm H} - 1)_{\mathbf{k}} \tag{91}$$

which is similar to Eq. (66) where the wavenumber is $k = \pi/L$.

Therefore, the diffusive modes are given by singular distributions instead of regular functions. The fractal character is related to the exponential instability in the microscopic dynamics.

In nonhyperbolic systems, diffusion may become anomalous in some regimes with a non-quadratic dispersion relation such as $s_k \simeq -C|k|^{\beta-1}$ $(2 < \beta < 3)$ and the corresponding modes are also singular [62].

C. Reaction-diffusion

We may also consider reaction-diffusion processes in the hard-disk periodic Lorentz gas in which the moving point particle carries a color A or B which changes with probability p_0 upon collision on some special disks called catalysts [10, 63–66]. The catalytic disks form a superlattice of the triangular lattice of hard disks. The reaction scheme is here:

$$A + \text{disk} \rightleftharpoons A + \text{disk} \tag{92}$$

$$B + \text{disk} \rightleftharpoons B + \text{disk} \tag{93}$$

$$A + \text{catalyst} \rightleftharpoons B + \text{catalyst}\,, \qquad \text{with probability } p_0 \tag{94}$$

The Liouvillian dynamics of such reaction-diffusion systems decouples into diffusion for the total density of particles and reaction for the difference between the densities of A and B particles. The diffusive sector precisely obeys the time evolution described in the previous subsection. On the other hand, the dispersion relation of the reactive modes are given by the following generalization of the van Hove formula [66]

$$s_{\mathbf{k}} = \lim_{t\to\infty} \frac{1}{t} \ln\langle (1-2p_0)^{N_t} \exp\left[i\mathbf{k}\cdot(\mathbf{r}_t - \mathbf{r}_0)\right]\rangle \tag{95}$$

where N_t is the number of catalysts met by the point particle during the time interval t. The dispersion relation (95) gives the leading Pollicott-Ruelle resonance of the time-evolution operator in the reactive sector. By expanding in powers of the wavenumber $\mathbf{k}$, we obtain

$$s_{\mathbf{k}} = -2\kappa - \mathcal{D}^{(\mathrm{r})}k^2 + O(k^4) \tag{96}$$

with the reaction rate

$$\kappa = -\lim_{t\to\infty} \frac{1}{2t} \ln\langle (1-2p_0)^{N_t}\rangle \tag{97}$$

and the reactive diffusion coefficient

$$\mathcal{D}^{(\mathrm{r})} = \lim_{t\to\infty} \frac{\langle (1-2p_0)^{N_t}(x_t - x_0)^2\rangle}{2t\langle (1-2p_0)^{N_t}\rangle} \tag{98}$$

assuming isotropy [66].

There exist two important regimes [65]:

The *rate-limited regime* is the regime where the reaction probability p_0 goes to zero. In this regime, the reaction rate to vanish as $\kappa = O(p_0)$, while the reactive diffusion coefficient converges to the diffusion coefficient itself: $\mathcal{D}^{(\mathrm{r})} = \mathcal{D} + O(p_0)$.

The *diffusion-limited regime* corresponds to the situation where the catalysts are so much far apart that the reaction is controlled by the diffusion time between the catalysts. In this case, the reaction rate behaves as [64]

$$\kappa \simeq (6.8 \pm 0.3)\, \frac{\mathcal{D}\, n_{\mathrm{c}}}{\ln \frac{n_{\mathrm{d}}}{n_{\mathrm{c}}}} \tag{99}$$

in a two-dimensional triangular periodic Lorentz gas with a density n_{d} of hard disks and a density n_{c} of catalysts.

The reactive modes are given by singular distributions with complex cumulative functions defined as [66]

$$F_{\mathbf{k}}(\theta) = \lim_{t\to\infty} \frac{\int_0^\theta d\theta' (1-2p_0)^{N_t(\theta')} \exp\left[i\mathbf{k}\cdot(\mathbf{r}_t - \mathbf{r}_0)_{\theta'}\right]}{\int_0^{2\pi} d\theta' (1-2p_0)^{N_t(\theta')} \exp\left[i\mathbf{k}\cdot(\mathbf{r}_t - \mathbf{r}_0)_{\theta'}\right]} \tag{100}$$

In the complex plane, these functions depict fractal curves of Hausdorff dimension D_{H} given by the root of the equation [66]

$$Q(D_{\mathrm{H}}, D_{\mathrm{H}}) = D_{\mathrm{H}} \operatorname{Re} s_{\mathbf{k}} \tag{101}$$

where $s_{\mathbf{k}}$ is the dispersion relation (95) of the reactive modes while the function in the left-hand side is defined as the following generalization of the Ruelle topological pressure (87):

$$Q(\alpha,\beta) \equiv \lim_{t\to\infty} \frac{1}{t}\ \ln\langle |1-2p_0|^{\alpha N_t} |\Lambda_t|^{1-\beta}\rangle \tag{102}$$

Therefore, the reactive modes as well as the diffusive modes present a singular character [66].

In conclusion, the singular character of the relaxation modes is directly related to the fact that these modes describe transient processes. We find here again the selection of trajectories associated with a given semigroup of time evolution and, thus, the breaking of the time-reversal symmetry. Here, the selection consists in weighting the trajectories according to the conditionally invariant complex measure. The relaxation modes of the forward semigroup are smooth in the unstable direction but singular in the stable direction. This singular character is of great importance in order to understand the production of entropy in these modes of relaxation, which is the purpose of the following section.

VII. ENTROPY PRODUCTION

A. *Ab initio* derivation of entropy production

In nonequilibrium thermodynamics, irreversibility is expressed by the production of entropy out of equilibrium. In order to verify that the previously constructed hydrodynamic modes are conform to this criterion, we have calculated the entropy production during a relaxation controlled by such a hydrodynamic mode of diffusion and showed that the

value expected from nonequilibrium thermodynamics is recovered. This verification has been carried out in a series of papers starting with the multibaker model of diffusion till general diffusive processes in multi-particle deterministic dynamical systems [10, 28–32]. This work has shown that, indeed, the singular character of the hydrodynamic modes of diffusion leads to a positive entropy production which precisely takes the value expected from nonequilibrium thermodynamics. Therefore, there is consistency between the existence of time-asymmetric singular modes and an irreversibility associated with an entropy production.

In order to evaluate the entropy production, we first have to introduce the partition the phase-space region $\mathcal{R}$ corresponding to the lattice cell $\mathbf{l}$ into phase-space cells $\{\mathcal{A}\}$ of equal volume and define the corresponding coarse-grained entropy:

$$S_t(\mathcal{R}|\{\mathcal{A}\}) \equiv -\sum_{\mathcal{A}\subset\mathcal{R}} \nu_t(\mathcal{A})\ \ln\frac{\nu_t(\mathcal{A})}{c^0} \tag{103}$$

where Boltzmann's constant is taken equal to unity, c^0 is a constant fixing the constant of entropy at equilibrium, and ν_t is the nonequilibrium measure at time t.

The time variation of the entropy over a time interval τ is given by the difference

$$\Delta^\tau S(\mathcal{R}|\{\mathcal{A}\}) = S_t(\mathcal{R}|\{\mathcal{A}\}) - S_{t-\tau}(\mathcal{R}|\{\mathcal{A}\}) \tag{104}$$

On the other hand, the *entropy flow* is defined as the difference between the entropy which enters the phase-space region $\mathcal{R}$ and the entropy which exits that region:

$$\Delta_{\rm e}^\tau S(\mathcal{R}|\{\mathcal{A}\}) \equiv S_{t-\tau}(\mathbf{\Phi}^{-\tau}\mathcal{R}|\{\mathcal{A}\}) - S_{t-\tau}(\mathcal{R}|\{\mathcal{A}\}) \tag{105}$$

Accordingly, the *entropy production* over a time τ is defined as

$$\Delta_{\rm i}^\tau S(\mathcal{R}|\{\mathcal{A}\}) \equiv \Delta^\tau S(\mathcal{R}|\{\mathcal{A}\}) - \Delta_{\rm e}^\tau S(\mathcal{R}|\{\mathcal{A}\}) \tag{106}$$

We here consider a large but closed system such as a periodic Lorentz gas in a large box. Since the system is mixing, the nonequilibrium weights of the cells $\{\mathcal{A}\}$ converge to their equilibrium values

$$\lim_{t\to\infty} \nu_t(\mathcal{A}) = \mu_{\rm eq}(\mathcal{A}) \tag{107}$$

The knowledge of the Pollicott-Ruelle resonances $s_{\mathbf{k}}$ and the associated eigenmodes $\Psi_{\mathbf{k}}$ and $\tilde{\Psi}_{\mathbf{k}}$ allows us to control the asymptotic approach to the equilibrium value:

$$\nu_t(\mathcal{A}) \simeq \int d\mathbf{k}\ \langle I_{\mathcal{A}}|\Psi_{\mathbf{k}}\rangle\ \exp(s_{\mathbf{k}}t)\ \langle\tilde{\Psi}_{\mathbf{k}}|p_0\rangle + \cdots\ \to_{t\to+\infty}\ \mu_{\rm eq}(\mathcal{A}) \tag{108}$$

where $I_{\mathcal{A}}(\mathbf{\Gamma})$ is the indicator function of the cell $\mathcal{A}$ and p_0 is the initial density. The integral is performed over the wavenumbers $\mathbf{k}$ of the first Brillouin zone of the lattice. By expanding in powers of the wavenumber $\mathbf{k}$, we have been able to show in Ref. [32] that the entropy production takes the expected value

$$\frac{1}{\tau}\Delta_{\rm i}^\tau S(\mathcal{R}|\{\mathcal{A}\}) \simeq \frac{\mathcal{D}}{n(\mathbf{l},t)}\ \left[\frac{\partial n(\mathbf{l},t)}{\partial\mathbf{l}}\right]^2 \tag{109}$$

in the long-time limit. In Eq. (109), $n(\mathbf{l},t)$ denotes the mean particle density in the lattice cell $\mathbf{l}$ corresponding to the phase-space region $\mathcal{R}$. This mean particle density converges to its uniform equilibrium value in the long-time limit: $\lim_{t\to\infty} n(\mathbf{l},t) = n_{\rm eq}$. In the same limit, the gradient of particle density decreases as the system approaches the thermodynamic equilibrium and the entropy production progressively vanishes according to Eq. (109) as expected by nonequilibrium thermodynamics. A remarkable feature is that the result (109) holds for a partition into arbitrarily small phase-space cells $\{\mathcal{A}\}$. This is due to the fact that the hydrodynamic modes of diffusion are singular down to arbitrarily small scales, which confers to the entropy production (109) an incomparable robustness.

The singular character of the hydrodynamic modes of diffusion is an essential ingredient to obtain the positive entropy production (109). The reason is that the diffusion coefficient in Eq. (109) is given in terms of the nonequilibrium steady states (NESS) of diffusion as

$$\mathcal{D} = -\langle v_x\rangle_{\rm neq} = -\langle v_x\Psi_{\mathbf{e}_x}\rangle_{\rm eq} = \int_0^\infty \langle v_x(0)v_x(t)\rangle_{\rm eq}\ dt \tag{110}$$

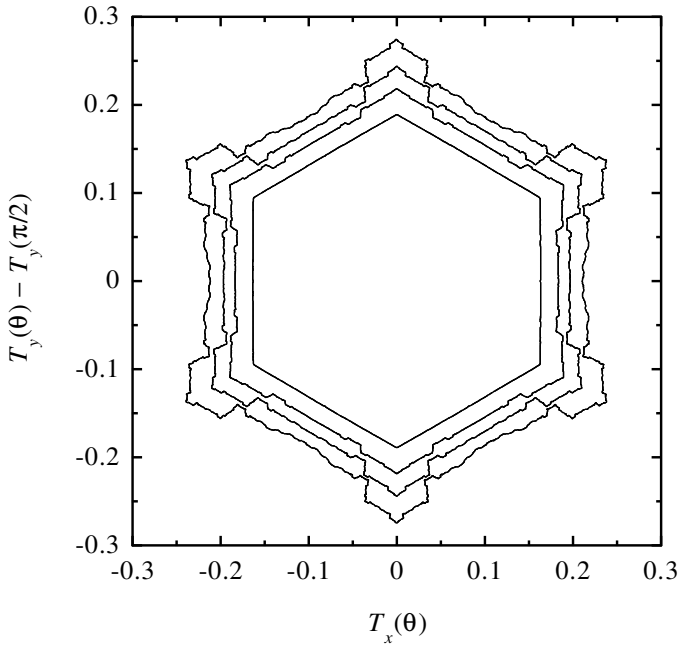

FIG. 7: Periodic hard-disk Lorentz gas: Curves of the cumulative functions of the NESS for triangular lattices of hard disks of unit radius with an intercenter distance of $d = 2.001, 2.1, 2.2, 2.3$ [44].

where v_x denotes the velocity of the tracer particle. The nonequilibrium steady state in Eq. (110)

$$\Psi_{\mathbf{g}}(\mathbf{\Gamma}) = \mathbf{g} \cdot \left[\mathbf{r}(\mathbf{\Gamma}) + \int_0^{-\infty} \mathbf{v}(\mathbf{\Phi}^t \mathbf{\Gamma}) dt \right] \tag{111}$$

appears by expanding the hydrodynamic modes of diffusion (82) at small wavenumbers [67]:

$$\Psi_{\mathbf{g}} = -i\, \mathbf{g} \cdot \frac{\partial \Psi_{\mathbf{k}}}{\partial \mathbf{k}}\Big|_{\mathbf{k}=0} \tag{112}$$

where $\mathbf{g}$ is the gradient of concentration. Finally, the Green-Kubo formula (110) is obtained from Eq. (111) because $\langle v_x x \rangle_{\rm eq} = 0$. We notice that Eq. (111) is the nonequilibrium steady state corresponding to a mean linear profile of concentration between two particle reservoirs which are arbitrarily far apart [10]. Because of Eq. (112), the singular character of the hydrodynamic modes is therefore transfered to the nonequilibrium steady state. From Eq. (111), it is clear that the NESS is singular because the unbounded random walk of the tracer particle makes the last term infinite. This singular character is hidden in the Green-Kubo formula because of the average with v_x, but it can be displayed in deterministic systems if v_x is replaced in Eq. (110) by an observable such as the indicator function of the curve $\mathbf{\Gamma}_\theta$ used to define the cumulative function (85) of the hydrodynamic modes. In doing so, we obtain the cumulative functions of the NESS also known as generalized Takagi functions:

$$T_{\mathbf{g}}(\theta) \equiv \int_0^\theta \Psi_{\mathbf{g}}(\mathbf{\Gamma}_{\theta'})\, d\theta' \tag{113}$$

The cumulative function $T_y(\theta) - T_y(\pi/2)$ corresponding to a gradient in the y-direction in the hard-disk periodic Lorentz gas is depicted versus the cumulative function $T_x(\theta)$ corresponding to a gradient in the x-direction in Fig. 7, where we observe the singular self-similar character [44].

These cumulative functions are smooth in the unstable phase-space directions but singular in the stable directions, which comes from the breaking of the time-reversal symmetry in the forward semigroup. As explained in Sec. II, there is no contradiction with the time-reversal symmetry of Newton's equations because of the selection of time-asymmetric trajectories in the construction of the semigroup.

B. Comparison with the second law of thermodynamics

The previous result shows that the coarse-grained entropy increases from the initial time when the initial probability distribution is prepared, up to its equilibrium value as $t \to +\infty$. The approach to the equilibrium value is performed at the rate of entropy production expected from nonequilibrium thermodynamics. The use of the eigenstates of the forward semigroup is essential for this result [28–32].

The coarse-grained entropy measures the disorder in the probability distribution down to the phase-space scale given by the size of the cells used in the coarse graining. Typically, the initial distribution has heterogeneities on large phase-space scales so that the initial entropy is lower than after some time evolution. Indeed, in mixing systems, the time evolution acts by deforming the initial probability distribution so that the heterogeneities are smoothed out in some phase-space directions but compressed in others. The heterogeneities do not disappear since the convergence toward the equilibrium state is only a weak convergence and not a strong one. Hence, the coarse-grained entropy reaches its equilibrium value after the heterogeneities have become smaller than the size of the cells of the coarse graining. This happens forward and backward in time so that the coarse-grained entropy has a similar increase forward and backward in time.

The increase backward in time should be excluded according to the second law of thermodynamics. This exclusion can be understood by referring to the problem of preparation of the initial conditions. As discussed in the introduction, the Newtonian scheme allows the preparation of arbitrary initial conditions in the phase space although the world is following a single trajectory from a unique initial condition in a far remote past. The preparation of specified initial conditions requires the use of a preparing device which is typically surrounding the system under study. This preparing device is not included in the description by Newton's equations of the subsystem under study. The preparation of the initial conditions involves processes taking in place in the preparing device which are also of relaxation type. We should therefore consider the coarse-grained entropy of the total system composed of the subsystem and the preparing device. The entropy of this total system can be expected to come from even lower values than its value at the instant when the initial condition of the subsystem is launched, in agreement with the second law of thermodynamics. Every time new initial conditions are prepared, the description should be enlarged to include the preparing device together with the subsystem. We have here the following regression: The consideration of a larger system pushes the choice of initial conditions backward in time allowing a lower entropy in a remoter past because the initial conditions of the larger system involve more degrees of freedom and are thus statistically more correlated in the past.

This reasoning leads us to impose the condition that *the phase-space cells used in the coarse-grained entropy must have a size smaller than the smallest heterogeneities of the initial probability distribution.* This condition is such that the coarse-grained entropy should remain constant as long as the time evolution does not refine the heterogeneities below the scale of the used phase-space cells, even for weird initial distributions with high statistical correlations down to some small phase-space scales. At long enough time, the coarse-grained entropy increases in conformity with the second law of thermodynamics and nonequilibrium thermodynamics, as shown here above. We should here mention that the phase-space cells used in the definition of the coarse-grained entropy can also be tailored to the dynamics of the system as proposed in Ref. [68].

VIII. NONEQUILIBRIUM STEADY STATES

A. Breaking the time-reversal symmetry at boundaries

Stationary states can be maintained out of equilibrium by imposing nonequilibrium constraints at the boundaries of an open system. These constraints induce fluxes of energy or matter across the system, leading to an irreversible entropy production.

Such nonequilibrium constraints can be considered as boundary conditions on the solutions $p(\mathbf{\Gamma}, t)$ of Liouville's partial differential equation (19). These boundary conditions are imposed to the probability density $p(\mathbf{\Gamma}, t)$ on some hypersurfaces in the phase space where the particles are incoming the system. These phase-space hypersurfaces correspond to the physical boundaries of the system in the three-dimensional world. Most of the trajectories of the full system enter in the phase-space domain delimited by these hypersurfaces and they spent in general a finite amount of time inside the domain before exiting. The average value of the time between entrance and exit is of the order of $1/(Avn)$ where A is the area of the container n is the density of particles, and v is the mean speed of the particles. This time is of the order of 10^{-29} second for air at room temperature and pressure in a container of 1 m^3. We notice that the number of particles inside the boundaries of the open system may fluctuate so that we may have to generalize the Liouville equation (19) into a hierarchy of Liouville's equations for the probability density $p^{(N)}$ of N particles

inside the system:

$$\partial_t \, p^{(N)} = \{H^{(N)}, p^{(N)}\} \tag{114}$$

with the global normalization

$$\sum_{N=0}^{\infty} \int p^{(N)} d^N\Gamma = 1 \tag{115}$$

and appropriate boundary conditions [10, 69].

Typically, the incoming trajectories are statistically uncorrelated while the outgoing trajectories are finely correlated according to the dynamics inside the system. Therefore, the incoming probability distribution is smooth with heterogeneities on spatial scales of the order of the macroscopic distances between the different thermostats or chemiostats at different temperatures or chemical potentials. In contrast, the outgoing probability distribution has extremely fine heterogeneities on tiny phase-space scales, reflecting the fine statistical correlations induced by the microdynamics internal to the system. After some transient time, a nonequilibrium steady state (NESS) establishes itself which is described by an invariant probability distribution.

Clearly, this invariant probability distribution is not time-reversal symmetric because the boundary conditions explicitly break the time-reversal symmetry [10, 67]. Distinct trajectories $\mathcal{C}$ and $\mathbf{\Theta}(\mathcal{C})$ have different probability weights in this invariant measure μ:

$$\mu(\mathcal{A}) \neq \mu\left[\mathbf{\Theta}(\mathcal{A})\right] \tag{116}$$

for the phase-space cells $\mathcal{A} \subset \mathcal{M}$ such that $\mathcal{A} \neq \mathbf{\Theta}(\mathcal{A})$. In contrast, the invariant probability distribution $\mu_{\rm eq}$ describing the thermodynamic equilibrium is time-reversal symmetric: $\mu_{\rm eq}(\mathcal{A}) = \mu_{\rm eq}\left[\mathbf{\Theta}(\mathcal{A})\right]$. Therefore, the boundary conditions required to define some NESS typically break the time-reversal symmetry.

B. The phase-space structure of NESS

An example of such NESS can easily be obtained for diffusion in an open Lorentz gas between two chemiostats or particle reservoirs at phase-space densities $p_\pm$ separated by a distance L. The phase-space density inside the system can only take either the value p_- corresponding to the reservoir on the left-hand side or p_+ from the reservoir on the right-hand side. In order to determine which value, we have to integrate the trajectory backward in time until the time of entrance in the system, $T(\mathbf{\Gamma}) < 0$. The value is p_- (resp. p_+) if the particle enters from the left-hand (resp. right-hand) side. If we denote by

$$\mathbf{g} = \frac{p_+ - p_-}{L} \, \mathbf{e}_x \tag{117}$$

the gradient of phase-space concentration, we can write the invariant density of the NESS in the form:

$$p_{\rm neq}(\mathbf{\Gamma}) = \frac{p_+ + p_-}{2} + \mathbf{g} \cdot \left[\mathbf{r}(\mathbf{\Gamma}) + \int_0^{T(\mathbf{\Gamma})} \mathbf{v}\left(\mathbf{\Phi}^t \mathbf{\Gamma}\right) dt \right] \tag{118}$$

Indeed, the integral of the particle velocity $\mathbf{v}$ backward in time until the time of entrance gives the position of entrance $\mathbf{r}(\mathbf{\Phi}^{T(\mathbf{\Gamma})}\mathbf{\Gamma}) = \pm L/2$ minus the current position $\mathbf{r}(\mathbf{\Gamma})$ which cancels the first term in the bracket. With the gradient (117), we end up with the result that

$$p_{\rm neq}(\mathbf{\Gamma}) = p_\pm \tag{119}$$

whether the trajectory enters from the left- or right-hand side [10].

The density of the NESS is a piecewise constant function with its discontinuities located on the unstable manifolds of the fractal repeller of the escape-rate formalism of Sec. V. Indeed, trajectories on the unstable manifold of the fractal repeller remain trapped between both reservoirs under the backward time evolution. The fractal repeller of the escape-rate formalism therefore controls the structure of the NESS. Its invariant density is very different from the one of the thermodynamic equilibrium but it remains absolutely continuous with respect to the Lebesgue measure as long as the reservoirs are separated by a finite distance L.

In the limit where the reservoirs are separated by an arbitrarily large distance L, the time of entrance goes to infinity: $T(\mathbf{\Gamma}) \to \infty$. If we perform this limit while keeping constant the gradient $\mathbf{g}$, the invariant density (118) is related to the density (111) according to

$$\Psi_{\mathbf{g}}(\mathbf{\Gamma}) = \lim_{L, p_+ - p_- = gL \to \infty} \left[p_{\rm neq}(\mathbf{\Gamma}) - \frac{p_+ + p_-}{2} \right] \tag{120}$$

Therefore, we reach the conclusion that the discontinuities on the unstable manifolds of the fractal repeller of the escape-rate formalism gives the singular character to the NESS as discussed in the previous Sec. VI. There is thus a deep connection between the fractal repeller of the escape-rate formalism, the fractal structure of the hydrodynamic modes, and the singular character of the NESS.

The results mentioned in Sec. VII show that the entropy production of the NESS (118) takes the value (109) expected from nonequilibrium thermodynamics as long as the phase-space cells chosen to define the coarse-grained entropy (103) remain larger than the phase-space size of the regions between the discontinuities of the density (118). Below this size the entropy production vanishes because of the absolute continuity of the invariant distribution of the NESS. However, in chaotic systems, the crossover size decreases exponentially fast with the separation L between the reservoirs so that nonequilibrium thermodynamics should hold down to extremely small scales in the phase space of diffusive systems only extending over a few dozens of mean free paths [10].

C. Entropy production and time-reversed entropy per unit time

Interesting relationships can be obtained by assuming that the nonequilibrium system has a (possibly approximate) Markovian description in terms of a master equation such as

$$\frac{d}{dt} p(\omega, t) = \sum_{\rho, \omega'} \left[p(\omega', t)\, W_\rho(\omega'|\omega) - p(\omega, t)\, W_{-\rho}(\omega|\omega') \right] \tag{121}$$

where $W_\rho(\omega|\omega')$ is the rate of the transition ρ between the states ω and ω' [70]. A reversed transition $-\rho$ is associated with each transition ρ. We suppose that the master equation admits a unique stationary solution. At the thermodynamic equilibrium, the stationary solution satisfies the conditions of detailed balance:

$$p_{\rm eq}(\omega')\, W_\rho(\omega'|\omega) = p_{\rm eq}(\omega)\, W_{-\rho}(\omega|\omega') \tag{122}$$

These conditions are in general not satisfied in NESS for which we have the more general conditions $(d/dt) p_{\rm neq}(\omega) = 0$. In a NESS, the entropy production is given by [71, 72]

$$\frac{1}{\tau} \Delta_{\rm i}^\tau S = \frac{1}{2} \sum_{\rho, \omega, \omega'} \left[p_{\rm neq}(\omega')\, W_\rho(\omega'|\omega) - p_{\rm neq}(\omega)\, W_{-\rho}(\omega|\omega') \right] \ln \frac{p_{\rm neq}(\omega')\, W_\rho(\omega'|\omega)}{p_{\rm neq}(\omega)\, W_{-\rho}(\omega|\omega')} \tag{123}$$

On the other hand, we can characterize the dynamical randomness in the NESS by considering the multiple-time probability

$$\mu_{\rm neq}(\omega_0 \omega_1 \omega_2 ... \omega_{n-2} \omega_{n-1}) \tag{124}$$

to observe stroboscopically the system in the states $\omega_0 \omega_1 \omega_2 ... \omega_{n-2} \omega_{n-1}$ at the successive times $t = 0, \tau, 2\tau, ..., (n-2)\tau, (n-1)\tau$. The dynamical randomness is characterized by the τ-entropy per unit time corresponding to this partition $\mathcal{P}$ into states $\{\omega\}$ and sampling time τ [9]:

$$h(\mathcal{P}, \tau) \equiv \lim_{n \to \infty} -\frac{1}{n\tau} \sum_{\omega_0 \omega_1 ... \omega_{n-1}} \mu_{\rm neq}(\omega_0 \omega_1 ... \omega_{n-1}) \ln \mu_{\rm neq}(\omega_0 \omega_1 ... \omega_{n-1}) \tag{125}$$

The dynamical randomness in the time-reversed path $\omega_{n-1} \omega_{n-2} ... \omega_2 \omega_1 \omega_0$ can be characterized by the time-reversed entropy per unit time [73]

$$h^{\rm R}(\mathcal{P}, \tau) \equiv \lim_{n \to \infty} -\frac{1}{n\tau} \sum_{\omega_0 \omega_1 ... \omega_{n-1}} \mu_{\rm neq}(\omega_0 \omega_1 ... \omega_{n-1}) \ln \mu_{\rm neq}(\omega_{n-1} ... \omega_1 \omega_0) \tag{126}$$

The difference between both entropies per unit time gives the entropy production in the NESS:

$$\frac{1}{\tau} \Delta_{\rm i}^\tau S = h^{\rm R}(\mathcal{P}, \tau) - h(\mathcal{P}, \tau) \geq 0 \tag{127}$$

in the limit $\tau \to 0$ [73]. The non-negativity is a consequence of the fact that the difference $h^{\rm R} - h$ between Eqs. (126) and (125) is a relative entropy which is known to be non-negative [74]. Equation (127) is a relationship between the entropy production and two characteristic quantities of the underlying dynamics. In particular, for a fine enough partition $\mathcal{P}$ and sampling time τ, the entropy per unit time $h(\mathcal{P},\tau)$ converges toward the Kolmogorov-Sinai entropy per unit time if this latter is well defined. Both $h^{\rm R}$ and h are given by large numbers but their difference gives the entropy production which is a quantity of the same order as those characterizing hydrodynamics. The relationship (127) says that the ratio of the multiple-time probabilities of a path and of a time-reversed path over a time interval $t = n\tau$ is given in terms of the irreversible entropy production $\Delta_{\rm i}^t S$ over the time $t = n\tau \to \infty$:

$$\frac{\mu_{\rm neq}(\omega_0\omega_1...\omega_{n-1})}{\mu_{\rm neq}(\omega_{n-1}...\omega_1\omega_0)} \simeq {\rm e}^{\Delta_{\rm i}^t S} \tag{128}$$

for $\mu_{\rm neq}$-almost all paths in the NESS. This relation explicitly shows that the breaking of the time-reversal symmetry in the NESS is directly related to the entropy production.

D. Entropy production and the fluctuation theorem

A fluctuation theorem can also be derived for Markovian processes described by the master equation (121) [19–23]. The breaking of detailed balance in the NESS is measured by the fluctuating quantity [20]

$$Z(t) \simeq \ln \frac{\mu_{\rm neq}(\omega_0\omega_1...\omega_{n-1})}{\mu_{\rm neq}(\omega_{n-1}...\omega_1\omega_0)} \tag{129}$$

The statistical moments of this quantity can be derived from the generating function

$$Q(\eta) \equiv \lim_{t\to\infty} -\frac{1}{t} \ln\langle {\rm e}^{-\eta Z(t)}\rangle \tag{130}$$

The use of such generating functions have been proposed for transport coefficients and other nonequilibrium properties in Refs. [10, 15, 75]. The fluctuation theorem says that the generating function (130) obeys the symmetry:

$$Q(\eta) = Q(1-\eta) \tag{131}$$

The quantity $Z(t)$ increases on average with a rate equal to the mean entropy production in the NESS so that

$$\frac{dQ}{d\eta}(0) = \lim_{t\to\infty} \frac{\langle Z(t)\rangle}{t} = \frac{d_{\rm i}S}{dt}\Big|_{\rm neq} \tag{132}$$

We can introduce the Legendre transform of the generating function as

$$R(\zeta) = \max_\eta \left[Q(\eta) - \zeta\ \eta\right] \tag{133}$$

which satisfies the identity

$$\zeta = R(-\zeta) - R(\zeta) \tag{134}$$

as a consequence of the symmetry (131). Since the function $R(\zeta)$ is the decay rate of the probability that $\frac{Z(t)}{t} \simeq \zeta$, we find that the ratio between the probabilities that $\frac{Z(t)}{t} \simeq \zeta$ and $\frac{Z(t)}{t} \simeq -\zeta$ behaves as

$$\frac{\mu_{\rm neq}\left[\frac{Z(t)}{t} \in (\zeta, \zeta + d\zeta)\right]}{\mu_{\rm neq}\left[\frac{Z(t)}{t} \in (-\zeta, -\zeta + d\zeta)\right]} \simeq {\rm e}^{\zeta t}\ , \qquad \text{for} \quad t \to +\infty \tag{135}$$

Here, we see that the time-reversal symmetry is explicitly broken by the invariant measure $\mu_{\rm neq}$ of the NESS. These results apply to nonequilibrium reactions [22].

Recently, the Schnakenberg analysis [71] of the graph of the Markovian process has allowed us to identify the affinities of the macroscopic nonequilibrium constraints on the system and to define the generating function of the nonequilibrium currents between the thermostats or chemiostats [23]. The Green-Kubo or Yamamoto-Zwanzig formulas as well as the Onsager and higher-order reciprocity relations can be derived from the fluctuation theorem for this generating function [23].

IX. QUANTUM SYSTEMS

A. Quantum Liouvillian resonances in infinite quantum systems

The idea that the Pollicott-Ruelle resonances can describe transient irreversible processes extends to many-body quantum systems which have a continuous spectrum. Examples of such systems includes the spin-boson systems and other system where a quantum subsystem is coupled to an infinite thermal bath [76]. Other examples are given by systems with many coupled spins [77].

In the case of a quantum subsystem coupled to a thermal bath such as the spin-boson model, the observables of the subsystem have a time evolution of relaxation type. It is possible to set up a quantum Liouvillian description in much the same spirit as the one described in Sec. III and to analyze the analytic continuation of the resolvent of the quantum Liouvillian operator, i.e., von Neumann's operator in the infinite-system limit. The resolvent may have different kinds of complex singularities including poles, which can thus be identified as quantum Liouvillian resonances analogue to the classical Pollicott-Ruelle resonances [76]. This programme has been successfully carried out for the spin-boson model of Hamiltonian:

$$\hat{H} \;=\; -\frac{\Delta}{2}\;\hat{\sigma}_z \;+\; \hat{H}_{\rm b} \;+\; \lambda\;\hat{\sigma}_x\;\hat{B} \tag{136}$$

where σ_x, σ_y, and σ_z are the Pauli matrices. The parameter Δ is the energy splitting between the two levels of the subsystem in absence of coupling to the reservoir, and λ is the perturbation parameter. The reservoir or thermal bath is a collection of harmonic oscillators of Hamiltonian

$$\hat{H}_{\rm b} \;=\; \frac{1}{2}\;\sum_{\alpha}\left(\hat{p}_\alpha^2 \;+\; \omega_\alpha^2\;\hat{q}_\alpha^2\right) \tag{137}$$

while the coupling between the two-level subsystem and the bath is described by the operator

$$\hat{B} \;=\; \sum_{\alpha}\;c_\alpha\;\hat{q}_\alpha \tag{138}$$

and characterized by the so-called spectral strength

$$J(\omega) \;=\; \sum_{\alpha}\;\frac{c_\alpha^2}{2\omega_\alpha}\;\delta(\omega-\omega_\alpha) \tag{139}$$

In the weak-coupling limit, the quantum resonances can be obtained by perturbation theory and they are given by the eigenvalues of the Redfield operator of the forward semigroup [78]. We obtain four eigenvalues

$$s \;=\; 0 \tag{140}$$

$$s \;=\; -g(\infty)+O(\lambda^4) \tag{141}$$

$$s \;=\; \pm i\left[\Delta+\frac{h(\infty)}{2}\right]-\frac{g(\infty)}{2}+O(\lambda^4) \tag{142}$$

The first eigenvalue corresponds to the invariant equilibrium state. The other ones describe exponential decays, $\exp(st)$. The second one is the decay of the populations of the two levels. The third and fourth eigenvalues describe the damped oscillations of the quantum coherences. The coefficients are given by with

$$g(\infty) \;=\; 4\lambda^2\int_0^\infty \cos\Delta t\;{\rm Re}\,C(t)\;dt = 2\pi\lambda^2 J(\Delta)\;\coth\frac{\Delta}{2k_{\rm B}T} \tag{143}$$

$$h(\infty) \;=\; 4\lambda^2\int_0^\infty \sin\Delta t\;{\rm Re}\,C(t)\;dt \tag{144}$$

in terms of the time correlation function of the bath

$$C(t)\equiv\langle\hat{B}(t)\hat{B}\rangle_{\rm eq} = \int_0^\infty d\omega\;J(\omega)\;\left(\coth\frac{\omega}{2k_{\rm B}T}\;\cos\omega t\;-\;i\;\sin\omega t\right) \tag{145}$$

The resonance spectrum of the backward semigroup is given by $\{-s\}$.

If a n-level quantum subsystem is coupled to a thermal bath, the Redfield operator should have n^2 eigenvalues s describing a time evolution $\exp(st)$. One of them corresponds to the equilibrium invariant state, $n-1$ to the decay of the populations of the n levels, and n^2-n to the damping of the quantum coherences. The $n-1$ decays of the population are real eigenvalues, while the n^2-n eigenvalues for the coherences form $\frac{n^2-n}{2}$ pairs of complex conjugated eigenvalues $s=-\gamma_{lm}\pm i\omega_{lm}$. In the weak-coupling limit, the imaginary part are given by the Bohr frequencies $\omega_{lm}=(E_l-E_m)/2$ of the unperturbed systems up to corrections of order λ^2.

Diffusive behavior of an electron moving on a chain coupled to a thermal bath can similarly be described in terms of quantum Liouvillian resonance depending on the wavenumber k of the diffusive modes [79].

Quantum Liouvillian resonances corresponding to exponential decays have also been observed in systems with many coupled quantum spins [77]. In such systems, the continuous spectrum comes from the infinitely many spins in the system in place of an external thermal bath.

B. Emergence of relaxation behavior in finite quantum systems

We may wonder under which conditions relaxation behavior which is the feature of a continuous spectrum emerges in finite quantum systems. The problem is here that finite quantum systems have necessarily a discrete energy spectrum and, as a consequence, a discrete Liouvillian spectrum given by the Bohr frequencies. There is here a great difference with respect to classical systems where the Liouvillian spectrum can be continuous even in finite mixing systems with two degrees of freedom such as the chaotic Sinai or Bunimovich billiards [1, 2].

In finite quantum systems, the discreteness of the spectrum implies the presence of almost-periodic oscillations after an early decay in the time evolution of the mean value of some observable starting from a nonequilibrium initial density matrix. The almost-periodic oscillations manifest themselves beyond the Heisenberg time which is proportional to the level density: $t_{\rm Heisenberg}=\hbar n_{\rm av}(E)$. If the spectrum is quasi-continuous, the level density can be dense enough so that the Heisenberg time is postponed after a very long time. In a recent study of a system where the thermal bath of bosons is replaced by a finite system defined in terms of Gaussian random matrices of $\mathcal{N}$ levels, it has been shown that the early decay before the Heisenberg time can be well described in the weak-coupling regime by a quantum master equation obtained by averaging over the Gaussian random matrix ensemble [80, 81]. The condition of validity is that the quantum system playing the role of the thermal bath should after a dense enough spectrum with a number of levels $\mathcal{N}>10/\lambda^2$ for $\lambda<0.3$. Below this value, the trajectories of the individual systems in the ensemble fluctuate too much for the average behavior to be representative. For $\lambda=0.1$, a few thousands of energy levels is enough to have an excellent description in terms of the quantum master equation [80, 81].

The classical relaxation behavior can also be reached in the semiclassical limit without coupling the system to a thermal bath [82]. This has been shown experimentally by Sridhar and coworkers who extracted the Pollicott-Ruelle resonances by statistical analysis of the scattering of microwaves on disk scatterers [83–85]. Indeed, the autocorrelation function in energy of the wave scattering cross-section has poles at the classical Pollicott-Ruelle resonances of the scatterer [86–89]. We here have an example of emergence of classical relaxation behavior out of the wave-mechanical underlying dynamics.

C. NESS in quantum systems

A NESS can be obtained if a quantum subsystem is coupled to several thermal baths at different temperature. Recently, it has been shown that such quantum NESS are singular in the sense that they belong to classes of states which are not equivalent to the state of thermodynamic equilibrium [90]. This singular character which appears in quantum NESS is very much reminiscent of the singular character we have described in the previous sections.

X. CONCLUSIONS

In this paper, we have tried to show that the thermodynamics of irreversible processes can be understood in terms of expansions which are asymptotic in time and valid for either $t>0$ (forward semigroup) or $t<0$ (backward semigroup). In classical dynamical systems, these asymptotic expansions use the Pollicott-Ruelle resonances and other singularities at complex frequencies. These resonances and other complex singularities are obtained by analytic continuation toward complex frequencies of the spectral functions given by the Fourier transform of the time correlation functions of the observables. For sufficiently unstable dynamics, the Pollicott-Ruelle resonances and other singularities are independent of the particular observables provided they belong to some classes of smooth enough test functions so that we can say that they are intrinsic to the dynamics of the system. They can be conceived as some kind of generalized eigenvalues

of the Frobenius-Perron operator or of its generator, the so-called Liouvillian operator. The imaginary part of the complex frequency $z = is$ leads to an exponential time behavior $\exp(st) = \exp(-izt)$. The analytic continuation toward the lower half of the complex plane with $\mathrm{Re}\, s = \mathrm{Im}\, z < 0$ defines the forward semigroup, while the backward semigroup is obtained by continuation toward the upper half-plane with $\mathrm{Re}\, s = \mathrm{Im}\, z > 0$. Starting with the unitary group evolution, we thus obtain a description which is splitted into two semigroups valid on distinct time semi-axes. In the case of diffusive processes, the diffusion equation is valid only for positive times and the anti-diffusion equation only for negative times. Therefore, the two equations never coexist and, moreover, the anti-diffusion equation can be excluded because of the amplification of errors in the preparation of a state violating the second law, which is related to the non-convergence of the expansion of the backward semigroup to positive times. This mechanism makes precise Boltzmann's explanation of irreversible processes as processes for which the time-reversal history is highly improbable.

We thus find a spontaneous breaking of the time-reversal symmetry in the statistical description of the transient relaxation toward the state of thermodynamic equilibrium. This breaking of the time-reversal symmetry can be interpreted by a selection of trajectories which are not time-reversal symmetric. This selection occurs for instance in the case of decay processes where the eigenstate associated with the leading Pollicott-Ruelle resonance is concentrated on the unstable manifolds of the non-wandering subset. Therefore, the decay at positive times uses an eigenstate or conditionally invariant measure made of trajectories which are selected by the dynamics and which are moreover non-symmetric under time reversal. Indeed, the time-reversal symmetry maps the unstable manifolds onto the stable manifolds which are physically distinct trajectories. A similar selection of trajectories occurs for the eigenstates describing the transient processes of the escape-rate formalism.

In the case of the hydrodynamic and other relaxation modes in infinite spatially periodic systems such as diffusion in the periodic Lorentz gases, the eigenstates of the forward semigroup are smooth along the unstable manifolds but singular in the stable directions. Here, the eigenstates are constructed by weighting selectively the different trajectories in order for the eigenstate to be conditionally invariant. The time-reversed eigenstates of the backward semigroup are singular in the unstable directions but smooth in the stable ones and are therefore qualitatively different from the eigenstates of the forward semigroup. Therefore, we have here also the breaking of the time-reversal symmetry, which can be connected to the thermodynamic criterion of irreversibility by calculating the entropy production and showing that it conforms to the value expected from nonequilibrium thermodynamics. The remarkable observation is here that this value is obtained because of the singular character of the hydrodynamic modes in agreement with the idea of selection of time-reversal non-symmetric trajectories.

As discussed in Sec. IX, the concept of resonance can be extended to quantum systems.

Moreover, in several diffusive deterministic systems, we have shown in great detail that the leading Pollicott-Ruelle resonance gives the dispersion relation of diffusion. In hyperbolic systems, the leading Pollicott-Ruelle resonance is related to quantities of the underlying dynamics such as the Lyapunov exponents, the Kolmogorov-Sinai entropy per unit time, as well as the fractal dimensions. Relationships have thus been obtained between the transport coefficients and the characteristic quantities of chaos. In the escape-rate formalism, the leading Pollicott-Ruelle resonance is the escape rate which is proportional to the transport coefficient and given by the difference between the sum of positive Lyapunov exponents and the Kolmogorov-Sinai entropy. For diffusion, we get [12, 13]

$$\mathcal{D}\left(\frac{\pi}{L}\right)^2 \simeq \gamma = \left(\sum_{\lambda_i>0} \lambda_i - h_{\mathrm{KS}}\right)_L \tag{146}$$

and for viscosity or other transport coefficients [14, 48]

$$\eta\left(\frac{\pi}{\chi}\right)^2 \simeq \gamma = \left(\sum_{\lambda_i>0} \lambda_i - h_{\mathrm{KS}}\right)_\chi \tag{147}$$

Very similar relationships (88)-(89) are obtained for the hydrodynamic modes of diffusion in the two-dimensional Lorentz gases where the dispersion relation $s_{\mathbf{k}}$ is also the leading Pollicott-Ruelle resonance [59]

$$\mathcal{D}k^2 \simeq -\mathrm{Re}\; s_{\mathbf{k}} = \lambda(D_{\mathrm{H}}) - \frac{h_{\mathrm{KS}}(D_{\mathrm{H}})}{D_{\mathrm{H}}} \tag{148}$$

For NESS, there are the boundary conditions which explicitly break the time-reversal symmetry by weighting selectively the incoming trajectories by statistically uncorrelated probabilities. Here, the entropy production can also be given in terms of the difference between two quantities characterizing the underlying dynamics [73]

$$\frac{1}{\tau}\Delta_{\mathrm{i}}^{\tau} S = h^{\mathrm{R}}(\mathcal{P}, \tau) - h(\mathcal{P}, \tau) \tag{149}$$

The similarity with the relationships of the escape-rate formalism is clear. In the right-hand side, the Kolmogorov-Sinai entropy is simply replaced by the τ-entropy per unit time of the partition $\mathcal{P}$, while the role of the sum of positive Lyapunov exponents is played by the time-reversed entropy per unit time. In the left-hand side, we recover an irreversible quantity which is here the entropy production of the NESS. Finally, it is worthwhile to point out that the fluctuation theorem in the form (134)

$$\zeta = R(-\zeta) - R(\zeta) \tag{150}$$

has again the same structure as Eqs. (146)-(149) with an irreversible quantity in the left-hand side and the difference between two decay rates of probabilities in the right-hand side [16–23]. All the relationships (146)-(150) are indeed large-deviation formulas for the statistical time evolution in nonequilibrium conditions. They all have the feature of giving an irreversible property as the difference of two large-deviation quantities such as the decay rates of multiple-time probabilities or the growth rates of phase-space volumes. Moreover, they are compatible with Liouville's theorem. The discovery of these new dynamical large-deviation properties is a major advance in nonequilibrium statistical mechanics during the last fifteen years.

Acknowledgments. The author thanks Professor G. Nicolis for support and encouragement in this research. The author and this research are financially supported by the National Fund for Scientific Research (F. N. R. S. Belgium).

---

[1] Ya. G. Sinai, Russian Math. Surveys **25**, 137 (1970).
[2] L. A. Bunimovich, Commun. Math. Phys. **65**, 295 (1979).
[3] L. A. Bunimovich, and Ya. G. Sinai, Commun. Math. Phys. **78**, 247, 479 (1980).
[4] N. I. Chernov, J. Stat. Phys. **88**, 1 (1997).
[5] Ya. G. Sinai, Int. J. Bifurc. Chaos **6**, 1137 (1996).
[6] Ch. Dellago, H. A. Posch, and W. G. Hoover, Phys. Rev. E **53**, 1485 (1996).
[7] H. van Beijeren, J. R. Dorfman, H. A. Posch, and Ch. Dellago, Phys. Rev. E **56**, 5272 (1997).
[8] P. Gaspard and H. van Beijeren, J. Stat. Phys. **109**, 671 (2002).
[9] P. Gaspard and X.-J. Wang, Phys. Rep. **235**, 291 (1993).
[10] P. Gaspard, *Chaos, Scattering and Statistical Mechanics* (Cambridge University Press, Cambridge UK, 1998).
[11] P. Gaspard, M. E. Briggs, M. K. Francis, J. V. Sengers, R. W. Gammon, J. R. Dorfman, and R. V. Calabrese, Nature **394**, 865 (1998).
[12] P. Gaspard and G. Nicolis, Phys. Rev. Lett. **65**, 1693 (1990).
[13] P. Gaspard and F. Baras, Phys. Rev. E **51**, 5332 (1995).
[14] J. R. Dorfman and P. Gaspard, Phys. Rev. E **51**, 28 (1995).
[15] P. Gaspard and J. R. Dorfman, Phys. Rev. E **52**, 3525 (1995).
[16] D. J. Evans, E. G. D. Cohen, and G. P. Morriss, Phys. Rev. Lett. **71**, 2401 (1993).
[17] G. Gallavotti and E. G. D. Cohen, Phys. Rev. Lett. **74**, 2694 (1995).
[18] G. Gallavotti, Phys. Rev. Lett. **77**, 4334 (1996).
[19] J. Kurchan, J. Phys. A: Math. Gen. **31**, 3719 (1998).
[20] J. L. Lebowitz and H. Spohn, J. Stat. Phys. **95**, 333 (1999).
[21] C. Maes, J. Stat. Phys. **95**, 367 (1999).
[22] P. Gaspard, J. Chem. Phys. **120**, 8898 (2004).
[23] D. Andrieux and P. Gaspard, *Fluctuation theorem and Onsager reciprocity relations*, preprint (2004).
[24] M. Pollicott, Invent. Math. **81**, 413 (1985).
[25] M. Pollicott, Invent. Math. **85**, 147 (1986).
[26] D. Ruelle, Phys. Rev. Lett. **56**, 405 (1986).
[27] D. Ruelle, J. Stat. Phys. **44**, 281 (1986).
[28] P. Gaspard, J. Stat. Phys. **88**, 1215 (1997).
[29] S. Tasaki and P. Gaspard, Theoretical Chemistry Accounts **102**, 385 (1999).
[30] S. Tasaki and P. Gaspard, J. Stat. Phys. **101**, 125 (2000).
[31] T. Gilbert, J. R. Dorfman, and P. Gaspard, Phys. Rev. Lett. **85**, 1606 (2000).
[32] J. R. Dorfman, P. Gaspard, and T. Gilbert, Phys. Rev. E **66**, 026110 (2002).
[33] H. H. Hasegawa and D. J. Driebe, Phys. Rev. E **50**, 1781 (1994).
[34] S. Tasaki and P. Gaspard, Bussei Kenkyu Research Report in Condensed-Matter Theory **66**, 23 (1996).
[35] P. Gaspard, G. Nicolis, A. Provata, and S. Tasaki, Phys. Rev. E **51**, 74 (1995).
[36] P. Gaspard and S. Tasaki, Phys. Rev. E **64**, 056232 (2001).
[37] S. Tasaki and P. Gaspard, J. Stat. Phys. **109**, 803 (2002).
[38] P. Dahlqvist, Phys. Rev. E **60**, 6639 (1999).
[39] J.-P. Eckmann and D. Ruelle, Rev. Mod. Phys. **57**, 617 (1985).

[40] H. Kantz and P. Grassberger, Physica D **17**, 75 (1985).
[41] L.-S. Young, Ergod. Th. & Dyn. Syst. **2**, 109 (1982).
[42] F. Ledrappier and L.-S. Young, Annals of Math. **122**, 509 (1985).
[43] Ya. B. Pesin, Russian Math. Surveys **32**, 55 (1977).
[44] P. Gaspard, Int. J. Mod. Phys. B **15**, 209 (2001).
[45] P. Gaspard and S. A. Rice, J. Chem. Phys. **90**, 2225, 2242, 2255 (1989).
[46] P. Cvitanović and B. Eckhardt, Phys. Rev. Lett. **63**, 823 (1989).
[47] P. Gaspard and D. Alonso Ramirez, Phys. Rev. A **45**, 8383 (1992).
[48] S. Viscardy and P. Gaspard, Phys. Rev. E **68**, 041205 (2003).
[49] P. Hänggi, P. Talkner, and M. Borkovec, Rev. Mod. Phys. **62**, 251 (1990).
[50] H. A. Kramers, Physica (Utretcht) **7**, 284 (1940).
[51] S. Chandrasekhar, Rev. Mod. Phys. **15**, 1 (1943).
[52] E. Helfand, Phys. Rev. **119**, 1 (1960).
[53] S. Viscardy and P. Gaspard, Phys. Rev. E **68**, 041204 (2003).
[54] T. Tél, J. Vollmer, and W. Breymann, Europhys. Lett. **35**, 659 (1996).
[55] I. Claus and P. Gaspard, Phys. Rev. E **63**, 036227 (2001).
[56] I. Claus, P. Gaspard, and H. van Beijeren, Physica D **187**, 146 (2004).
[57] P. Grassberger and I. Procaccia, J. Chem. Phys. **77**, 6281 (1982).
[58] L. Van Hove, Phys. Rev. **95**, 249 (1954).
[59] P. Gaspard, I. Claus, T. Gilbert, and J. R. Dorfman, Phys. Rev. Lett. **86**, 1506 (2001).
[60] D. Ruelle, *Thermodynamic Formalism* (Addison-Wesley, Reading MA, 1978).
[61] T. Gilbert, J. R. Dorfman, and P. Gaspard, Nonlinearity **14**, 339 (2001).
[62] S. Tasaki and P. Gaspard, Physica D **187**, 51 (2004).
[63] P. Gaspard and R. Klages, Chaos **8**, 409 (1998).
[64] I. Claus and P. Gaspard, J. Stat. Phys. **101**, 161 (2000).
[65] P. Gaspard and I. Claus, Phil. Trans. Roy. Soc. Lond. A **360**, 303 (2002).
[66] I. Claus and P. Gaspard, Physica D **168-169**, 266 (2002).
[67] S. Tasaki, and P. Gaspard, J. Stat. Phys. **81**, 935 (1995).
[68] G. Nicolis and C. Nicolis, Phys. Rev. A **38**, 427 (1988).
[69] P. Gaspard, in: P. Garbaczewski and R. Olkiewicz, Eds., *Dynamics of Dissipation*, Lectures Notes in Physics **597**, (Springer-Verlag, Berlin, 2002) pp. 111-164.
[70] G. Nicolis and I. Prigogine, *Self-Organization in Nonequilibrium Systems* (Wiley, New York, 1977).
[71] J. Schnakenberg, Rev. Mod. Phys. **48**, 571 (1976).
[72] Luo Jiu-li, C. Van den Broeck, and G. Nicolis, Z. Phys. B - Condensed Matter **56**, 165 (1984).
[73] P. Gaspard, *Time-reversed dynamical entropy and irreversibility in Markovian random processes*, to appear in J. Stat. Phys. (2004).
[74] A. Wehrl, Rev. Mod. Phys. **50**, 221 (1978).
[75] P. Cvitanović, P. Gaspard, and T. Schreiber, Chaos **2**, 85 (1992).
[76] V. Jakšić and C.-A. Pillet, J. Math. Phys. **38**, 1757 (1997).
[77] T. Prosen, Physica D **187**, 244 (2004).
[78] P. Gaspard and M. Nagaoka, J. Chem. Phys. **111**, 5668 (1999).
[79] M. Esposito and P. Gaspard, *Exactly solvable model of quantum diffusion*, preprint (2004).
[80] M. Esposito and P. Gaspard, Phys. Rev. E **68**, 066112 (2003).
[81] M. Esposito and P. Gaspard, Phys. Rev. E **68**, 066113 (2003).
[82] P. Gaspard, D. Alonso, and I. Burghardt, Adv. Chem. Phys. **90**, 105 (1995).
[83] W. Lu, M. Rose, K. Pance, and S. Sridhar, Phys. Rev. Lett. **82**, 5233 (1999).
[84] W. Lu, L. Viola, K. Pance, M. Rose, and S. Sridhar, Phys. Rev. E **61**, 3652 (2000)
[85] K. Pance, W. Lu, and S. Sridhar, Phys. Rev. Lett. **85** (2000).
[86] M. Khodas and S. Fishman, Phys. Rev. Lett. **84**, 2837 (2000).
[87] J. Weber, F. Haake, and P. Seba, Phys. Rev. Lett. **85**, 3620 (2000).
[88] F. Haake, *Quantum Signatures of Chaos* (Springer, Berlin, 2000).
[89] O. Agam, Phys. Rev. E **61**, 1285 (2000).
[90] V. Jakšić and C.-A. Pillet, J. Stat. Phys. **108**, 787 (2002).